Molecular behavior of HP1α and CENP-A throughout the cell cycle in living cells

大阪府立大学博士(応用生命科学)学位論文

Molecular behavior of HP1α and CENP-A throughout the cell cycle in living cells

(生細胞における細胞周期を通したHP1α とCENP-Aの分子動態解析)

中川　千雅

2015年

CONTENTS

ABBREVIATIONS

CENP-A	centromere protein A
DAPI	4’,6-diamidino-2-phenylindole
DMEM	Dulbecco’s modified Eagle’s medium
Dnmt	DNA methyltransferase
DsRed	*Discosoma* sp. red fluorescent protein
ECFP	enhanced cyan fluorescent protein
EGFP	enhanced green fluorescent protein
GFP	green fluorescent protein
HP1α	heterochromatin protein 1 alpha
MEM	Eagle's minimum essential medium
mKO	monomeric Kusabira-ishi orange fluorescent protein
PCNA	proliferating cell nuclear antigen

INTRODUCTION

Cell is a fundamental unit of all living things. The cell duplicates its contents for the cell proliferation, and divides them into two cells. In particular, DNA in each chromosome must be faithfully replicated, and be accurately distributed to the two daughter cells. Cell cycle is a series of process from the cell division to the following cell division. In eukaryote, the cell cycle is divided into G1, S, G2, and M phases (Fig. 1). DNA is synthesized in S phase, and chromosome segregation and cell division are occurred in M phase (mitosis and cytokinesis, respectively). G1 phase is first gap phase between the end of cytokinesis and the start of DNA synthesis, and is a preparation period of the DNA synthesis. G2 phase is second gap phase between the end of DNA synthesis and the start of mitosis, and is a preparation period of the chromosome segregation and cell division. Progression of the cell cycle is regulated by complexes of cyclin-dependent kinase (CDK) and cyclin [1]. Events of the cell cycle occur in the correct sequence. When early event of the cell cycle has not been completed, later event is delayed or arrested. At checkpoints, the order of cell cycle events is controlled by the monitoring of the conditions, such as DNA damage, DNA replication, and spindle attachment of chromosomes [2]. Incorrect progression of the cell cycle contributes to the severe diseases, such as developmental defects and cancer. Therefore, visualization of the progression of the cell cycle by using specific proteins and spatiotemporal observation of the molecular behavior of the proteins are important for understand life phenomena.

Components of the replication machinery such as DNA methyltransferase (Dnmt) 1 [3] and DNA ligase I [4] were localized to nuclear replication sites during S phase. Celis and Celis [5] presented a putative sequence of proliferating cell nuclear antigen (PCNA) staining during the cell cycle and proposed the division of S phase into early and late stages according to the localization of PCNA in fixed cells. Cardoso *et al*. [4] reported that GFP-fused DNA ligase I was localized at replication foci in living

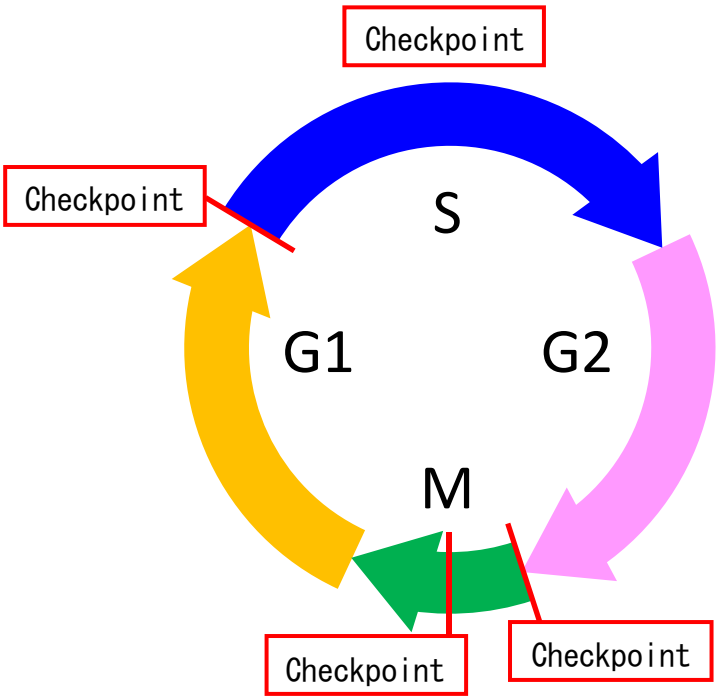

Fig. 1. Eukaryotic cell cycle.
In eukaryote, cell cycle is divided into G1, S, G2, and M phases. DNA is synthesized in S phase, and chromosome segregation and cell division are occurred in M phase (mitosis and cytokinesis, respectively). At checkpoints, the order of cell cycle events is controlled by the monitoring of the conditions, such as DNA damage, DNA replication, and spindle attachment of chromosomes. Main checkpoints are shown in G1/S, S, G2/M, M phase.

mammalian cells. Its characteristic redistribution enables entry into S phase to be monitored in living cells. Moreover, Easwaran *et al*. [6] reported that Dnmt 1 associates with replication foci throughout S phase and preferentially with heterochromatin during G2 and M phase. These authors [7] also reported that the combination of Dnmt 1 and DNA ligase I can be used as a marker of all cell cycle phases because their localizations are distinguishable between G1 and G2 phase. Similarly, GFP-PCNA can be used to perform automated cell cycle phase classification in living cells [8].

During the cell cycle, M phase is easily identified by the morphological changes of the cell such as mitosis and cytokinesis. However, the estimate of each phase in

interphase (G1, S, and G2 phases) needs the operation such as the observation of the protein that shows a distinct localization in the specific phase, or the measurement of DNA content. So far, the living cell marker throughout the cell cycle that can be easily used only by observing the specific localization of the protein is unknown. Therefore, the protein that changes the localization in interphase may be a candidate as a marker of all cell cycle phases.

In the present thesis, I have investigated the molecular behavior of the proteins that may change the localization in interphase in living cells. In CHAPTER I, I focus on heterochromatin protein 1α (HP1α) that localizes in the centromeric periphery. In CHAPTER II, I report the localizations of PCNA and centromere protein A (CENP-A) throughout interphase.

CHAPTER I

Visualization of the localization of HP1α throughout the cell cycle in living mouse cells and rhythmical flickering of heterochromatin dots in interphase

Heterochromatin was considered as a form of chromatin that remains condensed throughout the cell cycle and contains transcriptionally inactive genes. Heterochromatin protein 1 (HP1) is a non-histone chromosomal protein that was first identified in *Drosophila melanogaster* as a component of the chromocenter [9]. The *D. melanogaster* mutant, Su(var)2–5, is a dominant suppressor of position effect variegation (PEV) [10]. The fission yeast, *Schizosaccharomyces pombe*, also expresses a HP1 homolog called Swi6 [11] that plays a crucial role in the establishment and maintenance of heterochromatin. In higher eukaryotes, HP1a, HP1b and HP1c isoforms have been identified in *Drosophila* [12], and HP1α, HP1β, and HP1γ isoforms have been identified in mammals [13–15]. These isoforms contain two evolutionarily conserved domains, the chromo domain (CD) [16] at the N-terminus and the chromoshadow domain (CSD) [17] at the C-terminus.

Mammalian HP1α and HP1β are predominantly localized to centromere heterochromatin in interphase [14, 18, 19], while HP1γ is localized to both euchromatin and heterochromatin in interphase [20]. In mouse, *Mus musculus*, chromosomes except for the Y chromosome contain two types of satellite DNA repeats, minor satellite at the centric region and major satellite at the pericentric region [21, 22]. Major satellites are detected as large spots, and co-localize with the DAPI dense heterochromatin clusters in interphase mouse nuclei [23, 24]. HP1α is co-localized with major satellites domains, whereas minor satellites are juxtaposed but segregated from HP1α [24]. Sugimoto *et al.* [25] reported that a significant portion of HP1α dots has diffused in the nucleus in G2 phase and that the majority of HP1α further diffuses into the cytoplasm concomitant

with nuclear envelope breakdown, but some HP1α remains in the centromeres of mitotic chromosomes. However, it is not known when and how HP1α dots begin to diffuse in the nucleus of living cells. In addition, clarification of the molecular behavior of HP1α during the cell cycle may enable its use as a live cell marker for cell cycle progression. To elucidate the molecular behavior of HP1α throughout the cell cycle, I performed time-lapse imaging of two successive cell divisions in mouse C3H10T1/2 cell line stably expressing DsRed-HP1α [25].

MATERIALS AND METHODS

Stable cell lines.

For live-cell imaging, a murine mesenchymal stem cell line C3H10T1/2 expressing DsRed-HP1α, EGFP-CENP-A, and ECFP-histone H3 was used (provided by Professor Kenji Sugimoto, Osaka Prefecture University). pECFP-histone H3 and pTK-hyg [26] were introduced into the C3H10T1/2 cell line expressing DsRed-HP1α and EGFP-CENP-A [25] and stable transformants were selected in the presence of Hygromycin B (Roche Molecular Biochemicals, Mannheim, Germany) [27]. Cells were cultured in DMEM (Nissui Pharmaceutical, Tokyo, Japan) with 10% fetal bovine serum (PAA Laboratories GmbH, Pasching, Austria).

Live-cell imaging analysis.

Cells were inoculated into a 35 mm glass bottom dish (Iwaki, Funabashi, Chiba, Japan) and grown in an INUG2-ZILCS stage top incubator (Tokai Hit, Fujinomiya, Shizuoka, Japan). For a long-term multipoint time-lapse imaging, an Eclipse Ti-S fluorescent microscope (Nikon, Tokyo, Japan) was equipped with Plan Fluor 40X/NA 0.75 object lens (Nikon), a ProScanIII H117N1 XY-axis stage controller (Prior, Cambridge, UK), and a MAC5000 controller with excitation and emission filter wheels and a Z-axis motor (Ludl Electronic Products, Hawthorne, NY, USA). A 100W halogen

lamp was used as a light source to obtain the light of an appropriate wavelength at 57 μW [27]. The excitation and emission filters (572/28 and 632/60 nm, respectively) with a dichroic mirror (GFP/DsRed-A, Semrock, Rochester, NY, USA) were used. Time-lapse images (10 optical sections with 2 μm distance) at eight points were captured by an ImagEM C9100-13 CCD camera (Hamamatsu Photonics, Hamamatsu, Shizuoka, Japan) exposing for 300 ms at 6 min intervals, operating a Volocity software (ver. 5.3.3, Improvision, Coventry, UK). Pictures and movies were processed with a LuminaVision software for Mac OSX (Mitani Corporation, Fukui, Japan). Fluorescence intensity was measured with an ImageJ 1.42q software (National Institutes of Health, Bethesda, MD, USA).

RESULTS

Time-lapse analysis of DsRed-HP1α localization throughout the cell cycle.

HP1α was stably expressed as a fusion to DsRed in mouse C3H10T1/2 cells [25]. HP1α was localized to heterochromatin in interphase; however, the majority of DsRed-HP1α diffused in the nucleoplasm in G2 phase and further diffused into the cytoplasm in M phase. To precisely examine its diffusion pattern during the cell cycle, I performed long-term time-lapse imaging of C3H10T1/2 cells. Figure 2A shows representative fluorescent images of DsRed-HP1α in living cells at 30 min intervals after anaphase onset. After the first cell division (0 min), heterochromatin dots of HP1α were soon observed in small daughter cells in early G1 phase (30 min). Following the cell enlargement (60 min), the heterochromatin dots showed the typical localization of HP1α in interphase nuclei until 750 min. However, I noticed that HP1α began to diffuse into the nucleoplasm at around 750–780 min, and that the extent of its diffusion increased gradually until 1140–1170 min. HP1α had diffused further towards the nuclear periphery by 1890 min, and then became exclusively distributed in the nucleus (1920 min). The HP1α dots were hardly observed in the nucleoplasm and the cells entered into

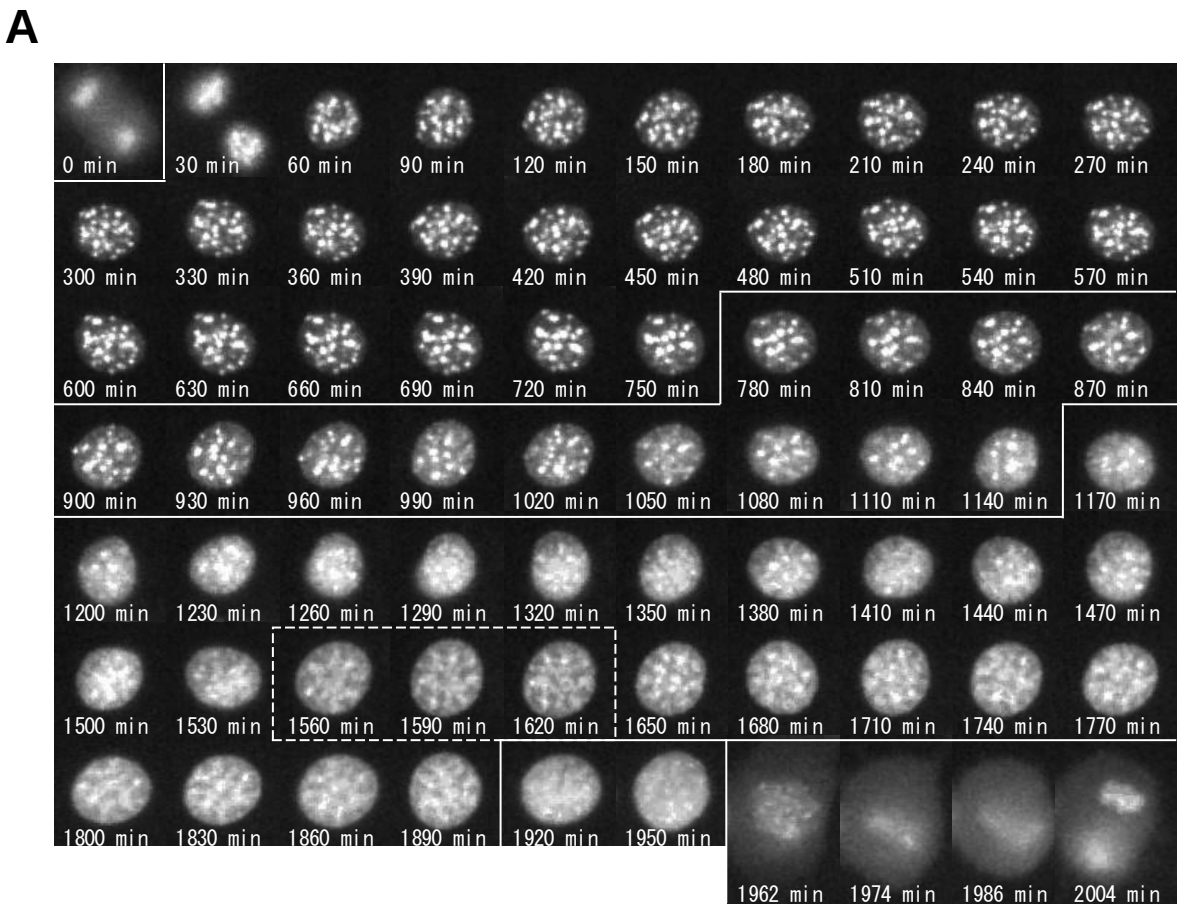

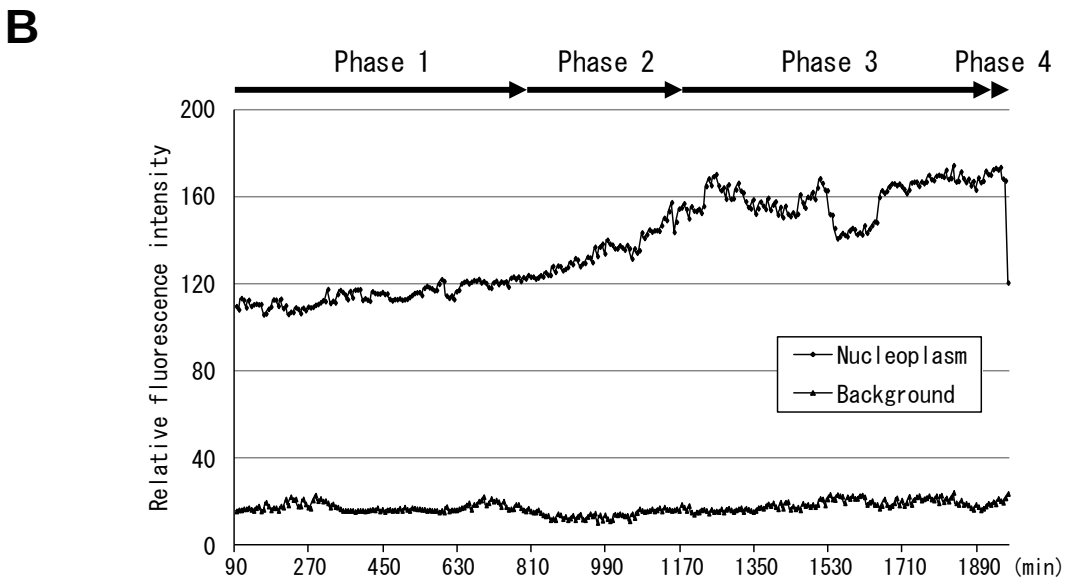

Fig. 2. For figure legend, see next page.

Fig. 2. Molecular behavior of DsRed-HP1α during the cell cycle of C3H10T1/2 cells.
A, Fluorescent images of a C3H10T1/2 cell through two successive cell divisions. Each image of C3H10T1/2 cells stably expressing DsRed-HP1α was captured at 6 min intervals. The elapsed time after anaphase of the first mitosis is indicated at the bottom. The second mitosis began after 1962 min. Only one of the daughter cells (lower right) is shown after 60 min. **B**, Fluorescence intensity of DsRed-HP1α following its diffusion into the nucleoplasm. The fluorescence intensity of nucleoplasm was measured at 6 min intervals and is indicated by arbitrary units. Note that the fluorescence intensity suddenly decreased at 1962 min, concomitant with nuclear envelope breakdown in the second mitosis. Segmentation of Phases 1–4 is shown at the top.

the second mitosis (1962 min).

According to the localization of DsRed-HP1α, I tentatively divided interphase into four phases (Phases 1–4). After the first cell division, HP1α formed heterochromatin dots in Phase 1 (30–750 min). HP1α began to diffuse into the nucleoplasm, and the extent of its diffusion increased gradually in Phase 2 (780–1140 min). HP1α diffused further towards the nuclear periphery in Phase 3 (1170–1890 min) and then uniformly into the entire nucleus in Phase 4 (1920–1950 min). Nuclear envelope breakdown occurred at 1962 min, resulting in the second cell division.

Figure 2B shows the fluorescence intensity of DsRed-HP1α in the nucleoplasm. Little change was observed in Phase 1, but the fluorescence intensity increased gradually in Phase 2 and reached a plateau in Phase 3. The increased rate of the fluorescence intensity in Phase 2 was 3.8-fold compared with that in Phase 1. The fluorescence intensity decreased at 1530 min and recovered at 1650 min, correlating with the enlargement of nuclear size in this period (see dotted area in Fig. 2A). The fluorescence intensity changed little in Phase 4 but rapidly decreased to the Phase 1 level (1962 min) concomitant with the collapse of the nuclear envelope. These results suggested that the fluorescence intensity of DsRed-HP1α was correlated with its distribution pattern in the cell cycle.

Interphase segmentation of C3H10T1/2 cells in the living state.

Next, I examined whether this cell cycle segmentation could also be applied to other HP1α-expressing individual cells. I followed two successive cell divisions of 10 independent cells in one experiment. I characterized the cell cycles of 14 daughter cells, eight of which were derived from the same parents (p1-2, p4-4, p6-1, and p6-3). Figure 3A shows typical images of these daughter cells in Phases 1–4, including the cell shown in Fig. 2A (p4-4-2). The counterpart daughter cell (p4-4-1) showed a similar distribution pattern of HP1α, as did another pair of daughter cells (p1-2-1 and p1-2-2).

After the first cell division, all daughter cells exhibited heterochromatin dots in Phase 1. The dots of p1-2-derived daughter cells were smaller than those derived from other cells, but with no significant difference between two daughter cells. The cell with small HP1α dots tended to have many number of HP1α dots. HP1α began to diffuse into the nucleoplasm in Phase 2. HP1α further diffused in Phase 3, such that each dot could not be easily distinguished. The fluorescence intensity of the nucleoplasm increased in Phase 3. HP1α diffused uniformly into the nucleoplasm in Phase 4, and was followed by the second cell division.

The average times of Phase 1, Phase 2, Phase 3, and Phase 4 were 11.4 ± 2.2 h, 5.3 ± 1.2 h, 12.4 ± 1.6 h, and 1.0 ± 0.3 h, respectively (n = 14). The length of the cell cycle varied from cell to cell, and from 25.5 h for the shortest (p1-2-2) to 34.5 h for the longest (p6-1-2). Although there was a significant difference between three pairs of daughter cells (25.5–31.5 h for p1-2, 28.2–34.5 h for p6-1, and 27.4–32.7 h for p6-3), the average was 30.1 ± 3.1 h (n = 14). These results are summarized in Fig. 3B, where the relative lengths of Phases 1–4 are illustrated as a percentage of the cell cycle. Interestingly, Phase 2 was estimated to be located in the middle of the cell cycle. Phase 4 started just before the second mitosis, probably in G2 phase, consistent with a previous report [25].

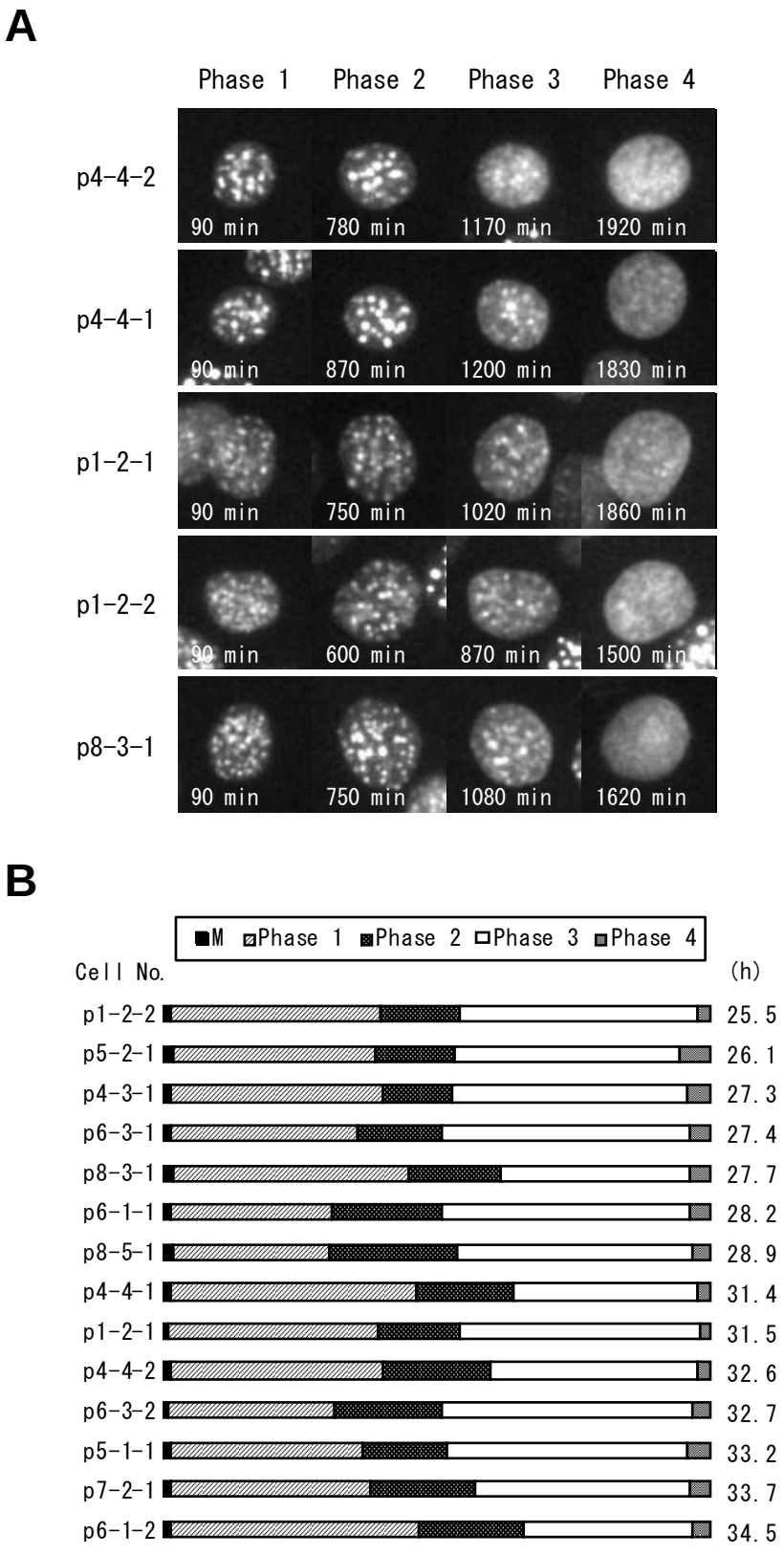

Fig. 3. For figure legend, see next page.

Fig. 3. Interphase segmentation of C3H10T1/2 cells.
A, Typical cell images of C3H10T1/2 cells in Phases 1–4. Interphase was divided into four phases by the pattern of DsRed-HP1α diffusion into the nucleoplasm. Heterochromatin dots of DsRed-HP1α were clearly observed 60 min after cell division (Phase 1). DsRed-HP1α began to diffuse into the nucleoplasm (Phase 2). The extent of DsRed-HP1α diffusion increased gradually and reached a plateau (see Fig. 2B). DsRed-HP1α diffused further towards the nuclear periphery (Phase 3) and uniformly diffused into the entire nucleoplasm (Phase 4). The elapsed time is indicated at the bottom. Each image from Phase 1 represents 90 min, by which time the heterochromatin dots were completely formed. Images of the start points of Phase 2 (600–870 min), Phase 3 (870–1200 min), and Phase 4 (1500–1920 min) are shown. **B**, Ratio of the four phases in the cell cycle of C3H10T1/2 cells. In the diagram, the cell cycle of 14 cells starts from the first mitosis (M). Times required for one cell cycle in each cell are shown on the right. Note that Phase 2 is roughly positioned in the middle of the cell cycle.

Periodic flickering of HP1α dots in Phase 2.

The diffusion of HP1α in the nucleoplasm started in Phase 2. Further observation revealed that the fluorescence intensity of HP1α dots changed periodically in Phase 2. Representative images of the flickering dots are shown in Fig. 4A. The insets show higher magnification images of the non-flickering and flickering dots in panels a and b, respectively. The dot in a square disappeared at 888 min, reappeared at 918 min, disappeared at 948 min and so on. I measured the fluorescence intensity of this dot every 6 min from 90 min through to 1086 min (Fig. 4B). The fluorescence intensity suddenly decreased at 798 min and recovered at 858 min. It decreased at 888 min and increased at 918 min and so on, as shown in Fig. 4A. This rhythmical cycle with intervals of about 30 min was observed five times until 1086 min.

I found that the flickering of the HP1α dots started at the beginning of Phase 2, concomitant with the initiation of HP1α diffusion at 756 min. The first and second upper peaks appeared at 60 min intervals, and the third and forth peaks appeared at 48 min intervals. The bottom peaks appeared at 72, 60, and 48 min intervals. The periodicity seemed to be steady at 48 min intervals after the third bottom peak. I could not follow this periodicity further, since the fluorescence intensity in the nucleoplasm was increased. When the time periods required for the increase and decrease of each

peak were compared, fluorescence recovery took longer than fluorescence lowering. In addition, the lowering period was rather constant and was estimated to be 30 min.

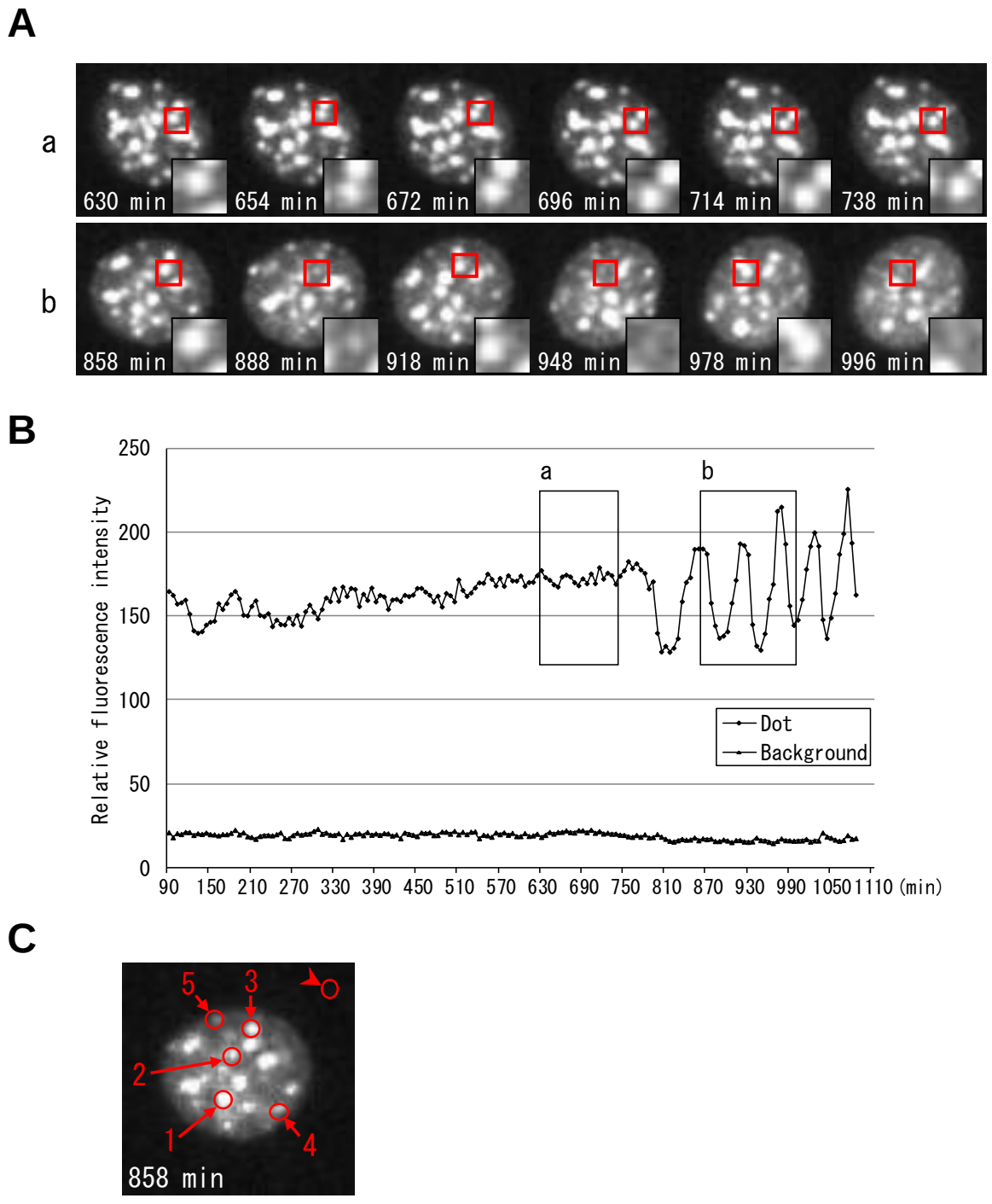

Fig. 4. For figure D and legend, see next page.

D

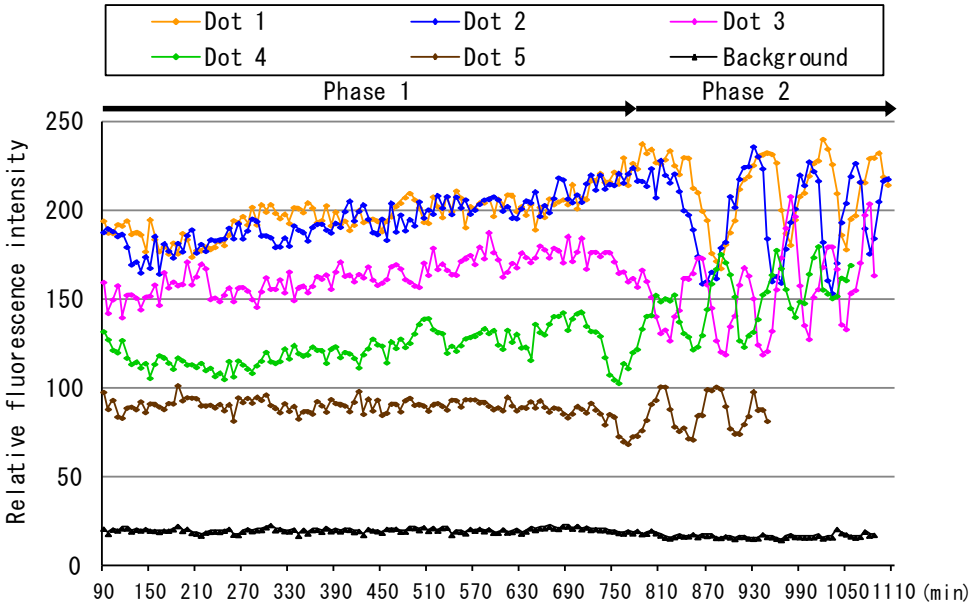

Fig. 4. Asynchronous periodic flickering of DsRed-HP1α dots in Phase 2.
A, Representative images of DsRed-HP1α dots in interphase nuclei in Phases 1 and 2. The relative positions of DsRed-HP1α dots did not change significantly between 630 and 738 min (a, Phase 1), but did between 858 and 996 min (b, Phase 2). The insets show higher magnification images of the HP1α dots marked with a square. Note that the HP1α dot in Phase 2 appears and disappears periodically with an interval of about 30 min. **B**, Fluorescence intensity of a DsRed-HP1α dot. The fluorescence intensity of the HP1α dot indicated with a square in Fig. A was measured at 6 min intervals. Each boxed area (a and b) corresponds to the cell panels in Fig. A. Note that the fluorescence intensity of HP1α suddenly changed at 780 min, concomitant with the beginning of Phase 2. The fluorescence intensity of this dot could not be measured after 1086 min. **C**, DsRed-HP1α dots applied for measurement of fluorescence intensity. Five DsRed-HP1α dots that flickered periodically are indicated with circles on the image captured at 858 min. The background intensity was also measured (upper right circle). **D**, Change in fluorescence intensity of HP1α dots. The fluorescence intensities of the DsRed-HP1α dots shown in Fig. C were measured at 6 min intervals. The first decreases in fluorescence intensity were observed at 756 (Dot 4), 768 (Dot 5), 822 (Dot 3), 864 (Dot 2), and 888 min (Dot 1), concomitant with the initiation of Phase 2 (780 min). Dots 1–5 showed a similar periodicity of flickering, although the fluorescence intensity of Dot 5 could not be followed after 948 min.

Asynchronous flickering of DsRed-HP1α dots in interphase nuclei.

To examine whether other HP1α dots also showed a similar periodicity of flickering in the same nucleus, I measured the fluorescence intensity of the 12 dots in a

cell. Figure 4C shows the live-cell imaging of p4-4-2 at 858 min in Phase 2, and representative 5 dots are indicated with arrows. As shown in Fig. 4D, all dots showed periodic flickering, although the initiation of flickering was different from dot to dot. The fluorescence intensity of Dot 1 decreased at 888 min, while that of Dot 4 decreased earlier than the others (756 min). Three to four peaks, at least, were observed for all dots. The flickering of Dots 1–5 continued to 1140 min (the end of Phase 2), but the fluorescence intensity could not be followed further, because of the further diffusion of HP1α in the nucleoplasm (see the Phase 3 cells in Fig. 3A). The flickering of the dots did not seem to be synchronous. The average time between the peaks of 5 dots was 35.1 ± 5.3 min. The periodic flickering was observed at 43% of the dots in this cell, and it was also observed at 39–48% of the dots in other cells (n = 4).

Visualization of cell cycle progression of C3H10T1/2 cells in living state.

When I observed this fluorescent C3H10T1/2 cells by long-term live-cell imaging, I could easily find the interphase cells in Phase 2 with periodic flickering of heterochromatin dots (Fig. 5A). Heterochromatin dots of DsRed-HP1α in a cell (No. 1) continued periodic flickering until 330 min, and diffused completely in nucleus at 480 min (Phase 4). The collapse of the nuclear envelope was observed at 510 min, followed by the mitosis and cell division. Similarly, another cell (No. 2) showed periodic flickering from 480 min to 750 min (Phase 2), and entered into Phase 4 at 1266 min. The collapse of the nuclear envelope was observed at 1326 min and the cell was divided into two daughter cells at 1362 min (Fig. 5B). After cell divisions, the daughter cells (No. 2A and No. 2B) enlarged in size in early G1 phase (1392–1410 min) and started periodic flickering at 2220 min and 2130 min, respectively, indicating that they entered into Phase 2. Thus, flickering of heterochromatin dots was a visual indication of Phase 2 and the complete diffusion of heterochromatin dots was another of Phase 4 in living C3H10T1/2 cells expressing DsRed-HP1α.

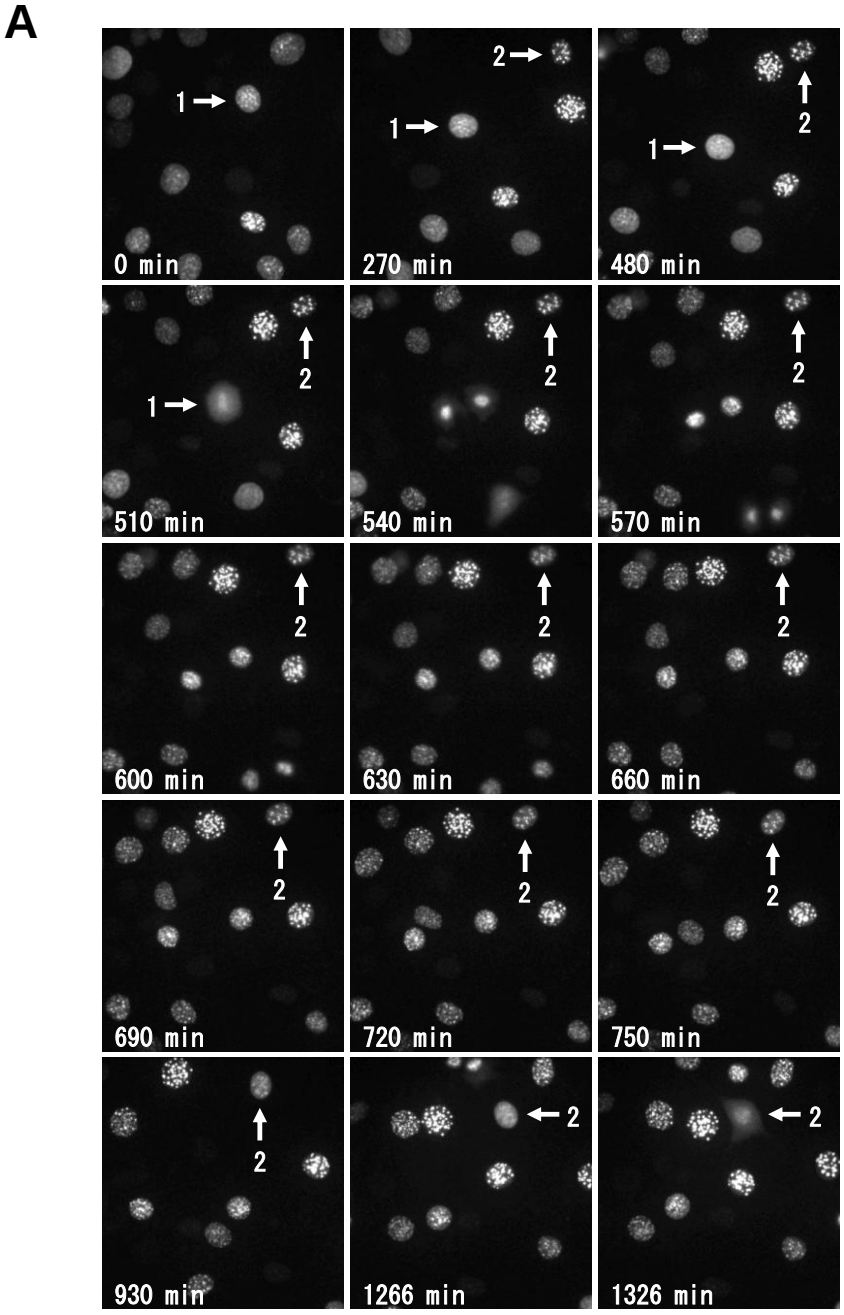

Fig. 5. Fate of interphase cells with flickering of heterochromatin dots.
Representative images of DsRed-HP1α in C3H10T1/2 cells by long-term live cell imaging. **A**, In cells observed flickering of heterochromatin dots, HP1α diffused throughout the entire nucleus, and progressed to M phase. The lower left corner of each image indicates the elapsed time. **B**, After cell division, heterochromatin dots of HP1α were soon observed in small daughter cells in early G1 phase. Following cell enlargement, the heterochromatin dots showed the typical localization of HP1α in interphase nuclei. Then, HP1α began to diffuse into the nucleoplasm and the dots started flickering with a rhythmical cycle. The lower left corner of each image indicates the elapsed time.

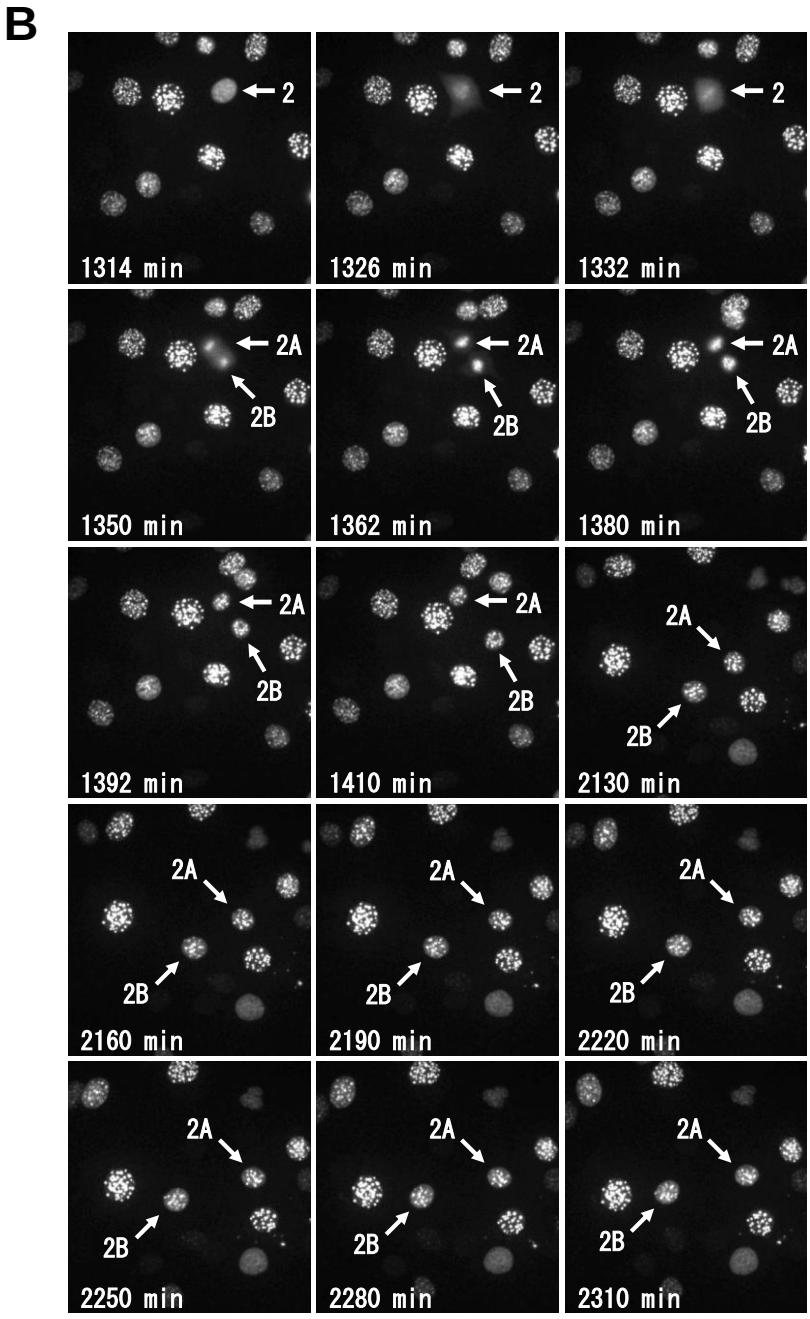

Fig. 5. (Continued)

The heterochromatin dots diffused completely in nucleus and then entered into M phase 10.4 ± 2.0 h (n = 5) later, after the flickering period, and the flickering of heterochromatin dots starts 10.4 ± 1.4 h (n = 3) later in the next cell cycle. As shown in Fig. 1, the average times based on the diffusion of HP1α of Phase 1, and Phase 3 plus Phase 4 were 11.4 ± 2.2 h and 13.5 ± 1.7 h, respectively (n = 14). I found that both

average times based on the periodic flickering of heterochromatin dots were similar to those based on the diffusion of HP1α.

DISCUSSION

In this Chapter I, I characterized the molecular behavior of heterochromatin dots throughout the cell cycle in mouse C3H10T1/2 cells. The diffusion of HP1α began at the midpoint of interphase and further progressed into the entire nucleus. The interphase was tentatively divided into four phases, Phases 1–4, by characterizing the localization of HP1α by the long-term live-cell imaging.

Figure 6 shows a schematic illustration of the localization of HP1α during the cell cycle. In Phase 1, HP1α formed heterochromatin dots soon after the first cell division, typical of its localization during interphase [18, 19, 25]. The localization of DsRed-HP1α seemed to be the same as that of EGFP-HP1α, although the tetrameric DsRed fusion tag may hinder the precise localization of the protein of interest [28]. In Phase 2, HP1α began to diffuse into the nucleoplasm and its diffusion increased gradually. In Phase 3, HP1α diffused further towards the nuclear periphery. In Phase 4, HP1α was uniformly distributed in the nucleus, and then the cells entered into M phase. In M phase, the majority of HP1α diffused into the cytoplasm but some remained in centromere heterochromatin, consistent with previous report [25].

The average length of the cell cycle was 30 h and apparently longer than non-fluorescent C3H10T1/2 cells. Similarly, other fluorescent protein fusions are known to extend the cell cycle length, especially in long-term time-lapse observations [27]. This cell cycle elongation is probably caused by, at least in part, the damage from the excitation light for fluorescent observation.

The fluorescence intensity of HP1α dots changed periodically in Phase 2 (Fig. 4B and D). The periodicity of the fluorescence of HP1α dots was not caused by the up-and-down movement of HP1α dots because I could not detect the fluorescence

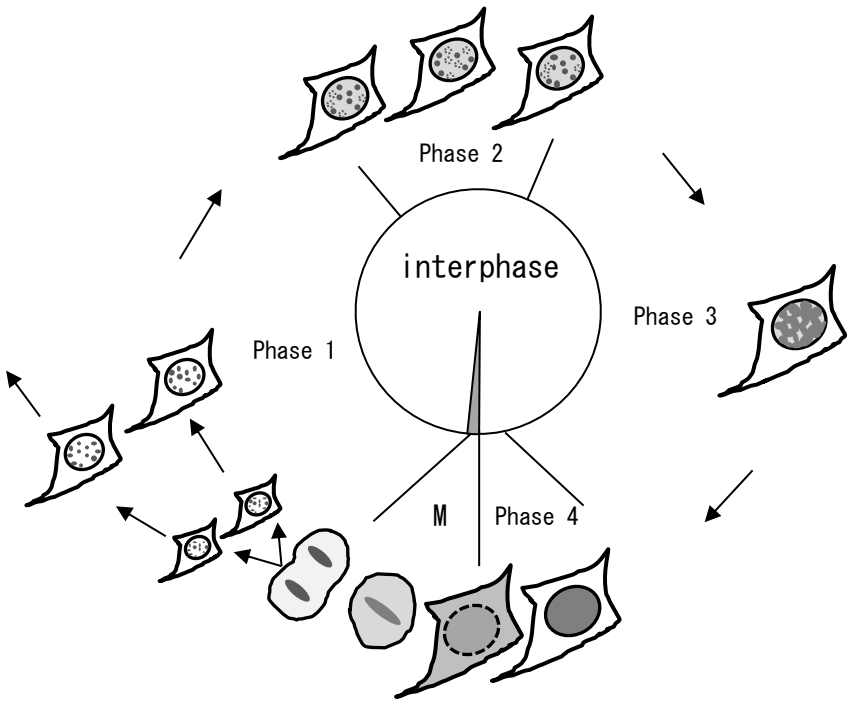

Fig. 6. Schematic illustration of the molecular behavior of HP1α during the cell cycle.
In Phase 1, HP1α formed heterochromatin dots in the nucleus after the first cell division. In Phase 2, HP1α began to diffuse in the nucleoplasm, and HP1α dots started flickering periodically. HP1α dots that disappeared because of periodic flickering are shown by the dotted circles. Note that periodic flickering of HP1α dots is asynchronous. In Phase 3, HP1α diffused further towards the nuclear periphery, and the HP1α dots became difficult to distinguish. In Phase 4, HP1α was distributed completely in the nucleus. In M phase (M), the majority of HP1α diffused into the cytoplasm but some remained in centromere heterochromatin [25].

among 10 Z axis slices with a distance of 2 μm. The flickering of HP1α dots with medium fluorescence intensity began with the start of HP1α diffusion, that is Phase 2 (Fig. 4B and D). Although I measured the fluorescence intensity of nucleoplasm containing the entire HP1α dot population (Fig. 2B), the fluorescence intensity increased independently of the periodic change in the fluorescence intensity of HP1α dots (Fig. 4B), suggesting that the diffusion of HP1α in the nucleoplasm was not caused by the degradation of HP1α dots but caused by the increase of the enhanced expression

of HP1α in the nucleoplsm. Thus, it may be better that I alternatively define Phase 2 as the period that the flickering of DsRed-HP1α starts and continues in live cell imaging. In fact, when I observed this C3H10T1/2 cell line in the living state, I could easily notice this phenomenon and know which cells were in Phase 2. In addition, I could tell that Phase 4 cells will soon enter into M phase and the flickering cells will proceed into Phase 4 in 11–15 h. So far, the molecular mechanism of periodic flickering of HP1α dots is unknown. Certain interaction between HP1α and major satellite DNA might be related in this phenomenon. It is likely that the flickering can be observed only in mouse cells, since heterochromatin dots are not so clearly recognized in other mammalian cells.

Sakaushi *et al.* [29, 30] reported that clathrin light chain a (CLCa) and Fes/CIP4 homology domain only 1 (FCHO1, also known as KIAA0290) showed periodic fluctuations at the *trans*-Golgi network in living cells. These periodic movements were suggested to be involved in clathrin-coated vesicle formation. Similarly, the periodic flickering of HP1α dots may be somehow correlated with the modification or conformation of HP1α [18], and/or interaction with other proteins, since HP1α is known to be associated with many proteins such as Suv39H1 [25], SNF2β [32], and histone H1.4 [33]. Interestingly, Schmiedeberg *et al*. [34] reported high- and low-mobility populations of HP1 in heterochromatin of mammalian cells. Krouwels *et al*. [35] also found the dynamic properties of SUV39H1 in mouse NIH3T3 living cells and suggested that a substantial population of SUV39H1 is immobile at heterochromatin and thus may play a structural role in heterochromatin structure. In addition, Dnmt 1 was interacted with Suv39h1-HP1 heterochromatin complex [36, 37]. The molecular interaction of HP1α with Suv39H1 and Dnmt 1 might be the molecular bases of periodic flickering of HP1α dots in interphase, consistent with the data of Stewart *et al.* [38].

CHAPTER II

Visualization of the localization of CENP-A throughout the cell cycle in living human cells and replication of DNA at centromere

The centromere is the chromosomal region of the kinetochore to which spindle microtubules attach during mitosis. Centromere identity is epigenetically determined and is assumed to be independent of the DNA sequence [40]. Centromere protein A (CENP-A) is a centromere-specific histone H3 variant [41] that replaces histone H3 in centromeric nucleosomes [42]. CENP-A was originally identified by anti-centromere autoantibodies [43], and was copurified with nucleosome core particles in human HeLa cells [44]. CENP-A-containing nucleosomes are distributed to daughter chromatids in S phase [45]. Histone H3.3 nucleosomes are deposited at the nucleosome gaps of newly synthesized centromeric DNA in S phase, and are replaced by CENP-A-containing nucleosomes in G1 phase [46].

Human CENP-A is assembled into prekinetochores in G1 phase, and is stably maintained through multiple cell divisions [45, 47]. Sugimoto *et al.* [48] reported the relative positions of CENP-A, CENP-B, and CENP-C in prekinetochores in interphase nuclei and in kinetochores of metaphase chromosomes in human MDA435 cells. In addition, these authors [25] characterized the molecular behavior of CENP-A and heterochromatin protein 1α (HP1α) during mitosis in living MDA435 cells. Recently, Lidsky *et al.* [49] reported the dynamics of Cid/CENP-A, CENP-C, and Cal 1 in *Drosophila* S2R+ cells, and presented images of live cells stably expressing Cid-EGFP and mCherry-PCNA throughout the cell cycle. However, the localization of human CENP-A throughout the cell cycle in living cells is unclear.

Proliferating cell nuclear antigen (PCNA) is one of the components of the DNA replication machinery that is conserved from yeast to mammals. In DNA synthesis, PCNA forms a homotrimer and encircles duplex DNA [50]. The localization of PCNA

changes in S phase according to the progression of DNA replication [5]. Chagin *et al*. [39] reported the progression of DNA replication throughout the cell cycle in living human HeLa cells stably expressing GFP-PCNA. PCNA is often used as an S phase marker in living cells [51, 52]. To elucidate the molecular behavior of human CENP-A throughout the cell cycle, I performed time-lapse imaging of HT1080 cells, with a modal number of 46 chromosomes [54], stably expressing mKO-CENP-A and EGFP-PCNA.

MATERIALS AND METHODS

Stable cell line.

For live-cell imaging, a human fibrosarcoma HT1080 cell line expressing mKO-CENP-A, EGFP-PCNA, and mPlum-histone H3 was used (provided by Professor Kenji Sugimoto, Osaka Prefecture University). Plasmid pmKO-CENP-A was constructed as previous report [53]. Plasmid pEGFP-PCNA was constructed by inserting the 0.7kb Xho I-BamHI fragment of plasmid pBluescript-PCNA into the Xho I-BamHI site of pEGFP-C1 (Clontech, Palo Alto, CA, USA), and plasmid pBluescript-PCNA was constructed by inserting the amplified DNA fragment encoding PCNA of pCMV6-XL5-PCNA (OriGene, Rockville, MD, USA) into the Xho I-BamHI site of pBluescript II SK(-) (Stratagene, La Jolla, CA, USA). Plasmid pmPlum-histone H3 was constructed by inserting the 0.4kb BamHI-EcoRI fragment of pECFP-histone H3 [26] into the BamHI-EcoRI site of pmPlum-C1. pmPlum-C1 was constructed by inserting the amplified DNA fragment encoding mPlum of pBAD-mPlum (provided by Professor Roger Y. Tsien, UCSD) into the Nhe I-Bgl II site of pEGFP-C1(Clontech). Plasmid pmPlum-histone H3 was introduced into the hunan fibrosarcoma HT1080 cell line [54] by electroporation as described previous report [48]. Stable transformant was selected in the presence of G418 disulfate (Nacalai Tesque, Kyoto, Japan). Next, plasmid mKO-CENP-A and plasmid pTK-Hyg (Clontech) were introduced into the cell

line HT1080 expressing mPlum-histone H3, and was selected in the presence of Hygromycin B (Roche Molecular Biochemicals, Mannheim, Germany). Then plasmid pEGFP-PCNA and plasmid pPUR (Clontech) were introduced into the cell line HT1080 expressing mPlum-histone H3 and mKO-CENP-A, and was selected in the presence of puromycin dihydrochloride (Sigma-Aldrich, St. Louis, MO, USA). Cells were cultured in MEM (Nissui Pharmaceutical, Tokyo, Japan) with 10% fetal bovine serum (PAA Laboratories GmbH, Pasching, Austria) at 37°C in 5% CO_2 atomosphere.

Live-cell imaging analysis.

Cells were inoculated into a 35 mm glass bottom dish (Iwaki, Funabashi, Chiba, Japan) and grown in an INUG2-ZILCS stage top incubator (Tokai Hit, Fujinomiya, Shizuoka, Japan). Time-lapsed images of HT1080 cells expressing mKO-CENP-A, EGFP-PCNA, and mPlum-H3 were captured essentially as described previous report [27]. For a long-term multipoint time-lapse imaging of EGFP-PCNA, an Eclipse Ti-S fluorescent microscope (Nikon, Tokyo, Japan) was equipped with Plan Apo 40X/NA 0.95 object lens (Nikon), a ProScanIII H117N1 XY-axis stage controller (Prior, Cambridge, UK), and a MAC5000 controller with excitation and emission filter wheels and a Z-axis motor (Ludl Electronic Products, Hawthorne, NY, USA). A 100W halogen lamp was used as a light source to obtain the light of an appropriate wavelength at 48 μW [27]. The excitation and emission filters (480/17 and 520/35 nm, respectively) with a dichroic mirror (Di01-R488/543/594, Semrock, Rochester, NY, USA) were used. Time-lapsed images (10 optical sections with 2 μm distance) at eight points were captured by an ORCA-ER CCD camera (Hamamatsu Photonics, Hamamatsu, Shizuoka, Japan) exposing for 300 ms at 3 min intervals, operating a Volocity software (ver. 5.3.3, Improvision, Coventry, UK). The Z-axis image stacks were converted to maximum -intensity projection. Pictures and movies were processed with a LuminaVision software for Mac OSX (Mitani Corporation, Fukui, Japan).

For a long-term multipoint time-lapse imaging of mKO-CENP-A and

EGFP-PCNA, an Eclipse Ti-S fluorescent microscope (Nikon) was equipped with Plan Apo VC 60X/NA 1.40 object lens (Nikon), a ProScanIII H117N1 XY-axis stage controller (Prior), and a MAC5000 controller with excitation and emission filter wheels and a Z-axis motor (Ludl Electronic Products). A 100W halogen lamp was used as a light source to obtain the light of an appropriate wavelength for mKO-CENP-A and EGFP-PCNA at 8 and 9μW, respectively [27]. The excitation and emission filters for mKO-CENP-A (543/3 and 572/28 nm, respectively) and used for EGFP-PCNA (480/17 and 520/35 nm, respectively) with a dichroic mirror (Di01-R488/543/594, Semrock) were used. Time-lapsed images (15 optical sections with 1 μm distance) at eight points were captured by an ImagEM CCD camera (Hamamatsu Photonics) exposing for 800 ms for mKO-CENP-A and 100 ms for EGFP-PCNA at 3 min intervals, operating a Volocity software (ver. 5.3.3, Improvision). The Z-axis image stacks were converted to maximum-intensity projection. Pictures and movies were processed with a LuminaVision software for Mac OSX (Mitani Corporation).

RESULTS

Time-lapse analysis of EGFP-PCNA localization throughout the cell cycle.

The localization of PCNA changes during S phase according to the progression of DNA replication [5, 39]. In addition, PCNA has been shown to localize throughout the nucleus except for the nucleoli (nucleolar exclusion) in early S phase [5, 39, 55]. To examine the molecular behavior of PCNA throughout the cell cycle, I first performed long-term time-lapse imaging of a human HT1080 cell line stably expressing EGFP-PCNA. I followed two successive cell divisions of three independent cells in one experiment. Figure 7A shows typical images of these cells and schematic illustrations of the localization of EGFP-PCNA. After the first cell division (0 min), PCNA was localized in the nucleus but excluded from the nucleoli in G1 phase. Many small foci of PCNA were distributed in the nucleus in early S phase. PCNA was localized around the

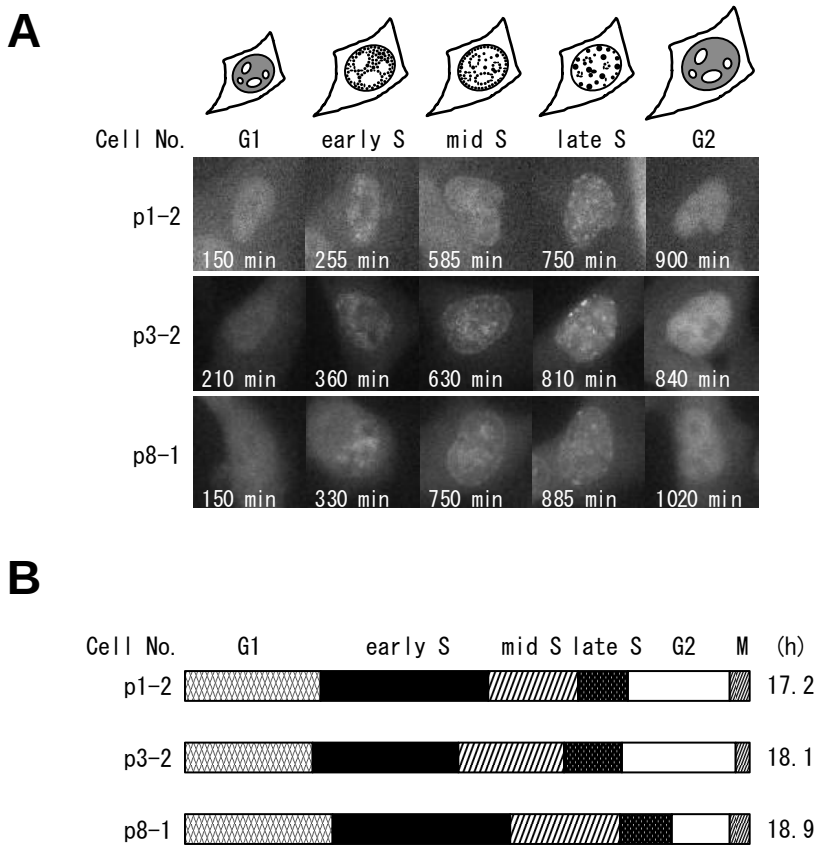

Fig. 7. Localization pattern of PCNA in living HT1080 cells during the cell cycle.
A, Time-lapsed images of three independent HT1080 cells expressing EGFP-PCNA. The typical localization pattern of PCNA is illustrated above the figure [5, 39, 55]. The elapsed time after cell division is shown at the bottom. **B**, Bar presentation of the cell cycle of three independent cells. Each phase in the cell cycle was estimated from the time-lapsed images above. Times required for one cell cycle in each cell are shown on the right.

nucleoli and in the nuclear periphery in mid S phase. Several large foci were observed in the nucleus in late S phase. PCNA was distributed in the nucleus with the exception of the nucleoli again in G2 phase. The localization pattern of PCNA in the nucleus was similar among p1-2, p3-2, and p8-1 cells.

The relative lengths of each phase of these cells are illustrated as a percentage of the cell cycle in Fig. 7B. The average times of G1, S, G2, and M phases were 4.4 ± 0.5

h, 10.2 ± 1.0 h, 2.9 ± 0.8 h, and 0.6 ± 0.1 h, respectively (n = 3). S phase was further divided into three phases according to the localization of PCNA [5], and the average times of early S, mid S, and late S phases were 5.3 ± 0.6 h, 3.3 ± 0.6 h, and 1.7 ± 0.2 h, respectively (n = 3). The average time of the cell cycle was 18.0 ± 0.9 h (n = 3).

These results showed that PCNA could be used as an S phase marker to follow the cell cycle progression of living human HT1080 cells and that the position of nucleoli could be estimated by the "nucleolar exclusion" pattern of interphase nuclei.

Time-lapse analysis of mKO-CENP-A and EGFP-PCNA localization throughout the cell cycle.

Human CENP-A assembles into kinetochores in G1 phase, and is stably maintained through multiple cell divisions [45, 47]. However, the localization of CENP-A in the cell cycle has not been well characterized in living cells. To elucidate the molecular behavior of CENP-A throughout the cell cycle, I performed long-term time-lapse imaging of a HT1080 cell line stably expressing mKO-CENP-A and EGFP-PCNA. Figure 8 shows representative fluorescent images of CENP-A and PCNA from M phase of the first cell division to the next M phase of the second cell division.
First, I characterized the localization of PCNA in the cell cycle. PCNA was distributed in the cytoplasm in M phase, but the fluorescence of PCNA was weaker in the region where CENP-A was localized (-3 min). After the cell division, PCNA was distributed in the nucleus as well as in the cytoplasm for 30 min and then gradually concentrated into the nucleus. Interestingly, I noticed the "nucleolar exclusion" pattern in four areas in the nucleus at 60 min (enclosed with white lines). These weak fluorescent areas of PCNA could be observed in the subsequent cell images of late G1 phase as well as early S phase (360–600 min). The relative positions of these areas were maintained in the nucleus until 720 min (see Fig. 9B for a reference). These observations indicated that PCNA was localized in the nucleoplasm except for the nucleoli from early G1 phase through to early S phase, consistent with the previous report [5, 39, 55].

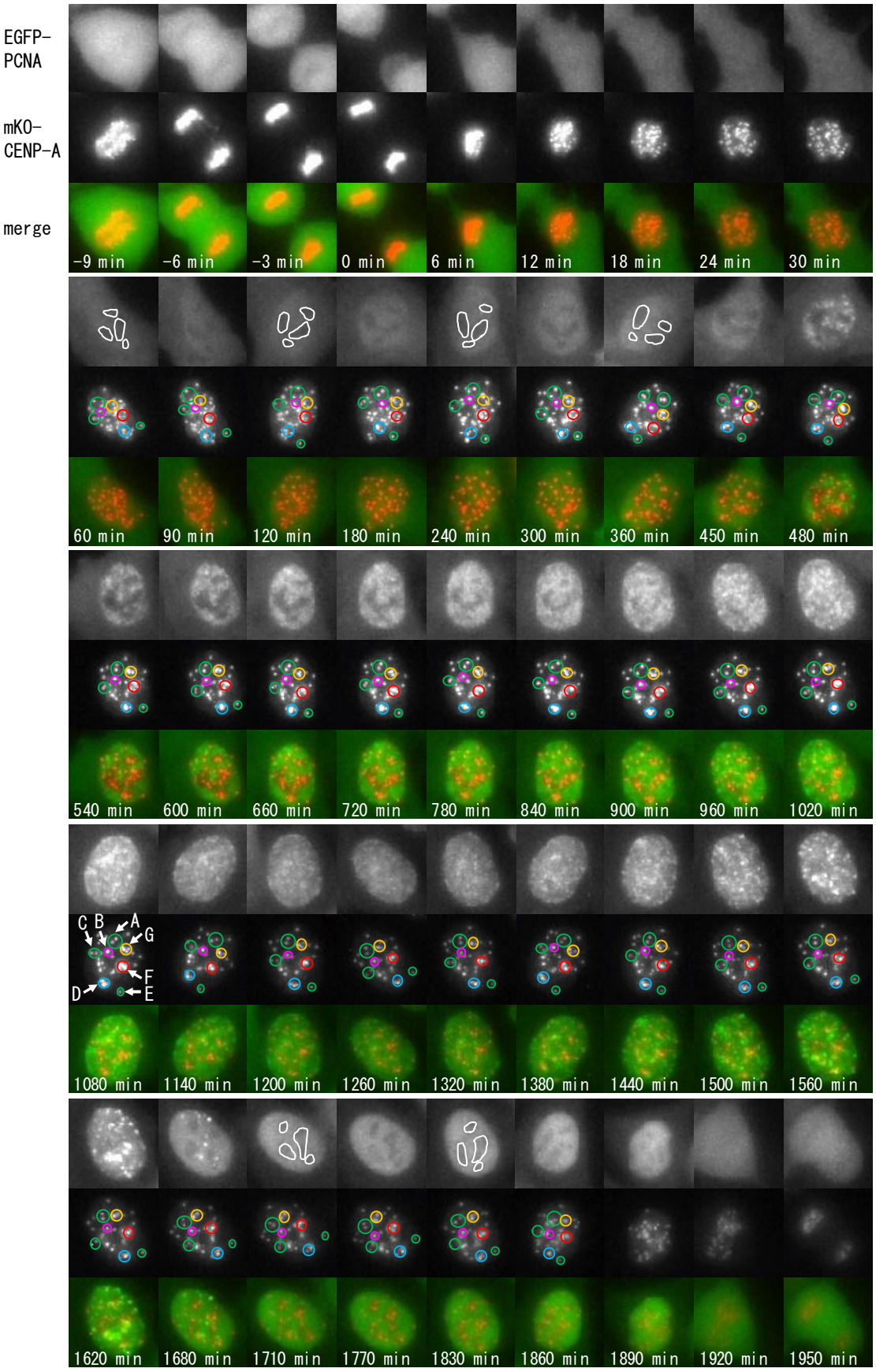

Fig. 8. For figure legend, see next page.

Fig. 8. Molecular behavior of mKO-CENP-A and EGFP-PCNA in HT1080 cells throughout the cell cycle.
Fluorescent images of a HT1080 cell through two successive cell divisions. Each image of a HT1080 cell stably expressing mKO-CENP-A (orange) and EGFP-PCNA (green) was captured at 3 min intervals but only the representative images are shown here. The elapsed time before or after G1 phase onset (0 min) is indicated at the bottom. Only the images of the lower daughter cell are shown after 6 min.

The S phase onset was identified at 480 min when replication foci of PCNA appeared. Many small foci of PCNA were distributed in the nucleus except for the nucleoli (480–660 min), so called "granular pattern" in early S phase [5]. The weak fluorescent areas of PCNA in the nucleus gradually decreased in size (720–900 min), and were hardly recognized after 1080 min. PCNA was also localized to the nuclear periphery after 1020 min (mid S phase). There was a drastic change in the distribution pattern of PCNA after 1500 min. Distinct foci were found in the nuclear periphery and large aggregates appeared in the nucleus at 1560–1620 min (late S phase). When most PCNA foci disappeared in the nucleoplasm at 1680 min, the nucleolar exclusion pattern was observed again. I assigned the end of late S phase at 1680 min. The weak fluorescent areas of PCNA could be observed in the subsequent cell images in G2 phase and the relative positions of these areas were maintained in the nucleus until 1830 min (enclosed with white lines), just before chromosome condensation (1890 min).

I next characterized the localization of CENP-A dots during the cell cycle. CENP-A dots were separated to the opposite poles at anaphase (-3 min). After cytokinesis, CENP-A dots were condensed in the daughter nuclei at 6 min. The distance between CENP-A dots gradually increased as the daughter nuclei grew in size at 6–30 min (early G1 phase). Most CENP-A dots were distinctly observed at 60 min. When I carefully compared the distribution patterns of CENP-A dots from G1 phase until G2 phase, I noticed that the relative positions of CENP-A dots were remained mostly unchanged throughout interphase. For an example, when seven groups of CENP-A dot(s) enclosed with colored circles were focused at 540 min (early S phase), I could

easily follow them by comparing the relative positions of colored circles in the subsequent cell images of 600 min, 660 min, 720 min and so on, until 1020 min (mid S phase).

Similarly, I could trace the relative positions of these CENP-A dots in G1 phase (60–450 min). Interestingly, I noticed that CENP-A dots enclosed with cyan, red, and orange circles were located in the less fluorescent areas of PCNA (enclosed with white lines in the upper panel at 60, 120, 240, and 360 min), while those enclosed with green and magenta circles were outside of these areas.

I further confirmed that the relative positions of these CENP-A dots were maintained from mid S phase through to late G2 phase. The seven groups of CENP-A dots enclosed by colored circles are indicated with A–G at 1080 min. Four groups (A, B, C, and G) were located in the upper half of the nucleus, while two groups (D and E) were located in the lower part and group F stayed in the middle of the nucleus. Their relative positions were maintained until 1860 min, just before chromosome condensation (1890 min). These results suggested that the relative positions of CENP-A dots changed little in interphase nuclei and certain CENP-A dots located at the nucleolar regions.

Localization pattern of the prekinetochore dots of mKO-CENP-A throughout the cell cycle.

To precisely determine the location of each CENP-A dot throughout the cell cycle, I re-analyzed the Z-stacks of the images at each time point from 60 min to 1830 min. Figure 9A shows the enlarged image of mKO-CENP-A at 1080 min. I identified and numbered 36 CENP-A dots. Four dots in cyan (17–20), five dots in orange (22–26), and eight dots in red circles (29–36) were localized in the less fluorescent areas of PCNA, corresponding to the nucleoli, at 480 min (see circles D, G, and F in Fig. 8). The dots in the yellow circle had also been localized in another nucleolar region at 480 min, but dot 10 (magenta triangle) was not localized to this region. In contrast, 12 dots in green

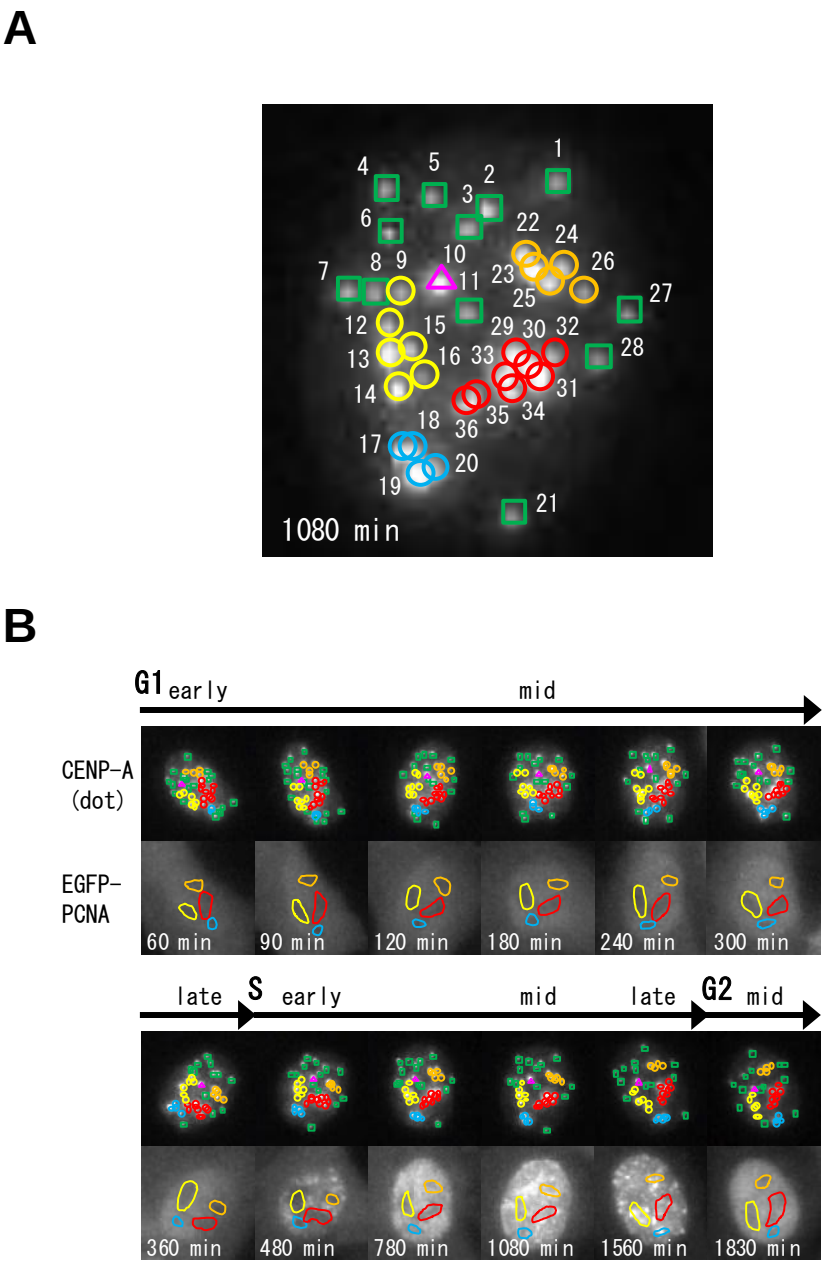

Fig. 9. Schematic presentation of the localization patterns of CENP-A dots during the cell cycle.
A, Identification of CENP-A dots in HT1080 cell at 1080 min. CENP-A dots were analyzed by the Z-stacks of the images at 1080 min and numbered from 1 to 36. Those localized in the nuclear periphery are shown by green squares and magenta triangle, and those in the nucleoli are shown by yellow, cyan, orange, and red circles. **B**, Localization pattern of CENP-A dots in HT1080 cell during the cell cycle. Most CENP-A dots observed at 1080 min were chased up to early G1 phase (60 min) and shown in the same color as identified by their positions at 1080 min. The boundaries of the presumptive nucleoli are enclosed in yellow, red, orange, and cyan lines (from large to small ones). The positions of presumptive nucleoli in mid and late S phases were estimated by the localization of CENP-A dots.

squares were localized in the nuclear periphery, including dot 11 in the center of the XY plane image of the nucleus.

The upper panels of Fig. 9B show a schematic presentation of the localization pattern of the CENP-A dots throughout the cell cycle. The lower panels show the boundary of four presumptive nucleoli, identified as less fluorescent areas of PCNA in the nucleus. When I chased all CENP-A dots from late G1 phase (360 min) to early G1 phase (60 min), CENP-A dots were localized in the nucleoli, except for a few dots (17, 19) in cyan located in the vicinity of the nucleus periphery. The presumptive nucleoli in mid and late S phases were estimated by the localization of CENP-A dots that had been placed there in G1 and early S phases. Interestingly, CENP-A dots enclosed with cyan, red, yellow, and orange circles were located in the less fluorescent areas of PCNA again in mid G2 phase. These results indicated that CENP-A dots occupied their own territory in the nucleus and that some CENP-A dots were at or close to the nucleoli in interphase nuclei, as described by Németh *et al.* [56].

Co-localization of mKO-CENP-A and EGFP-PCNA in mid and late S phases.

CENP-A-associated DNA was shown to replicate in mid-to-late S phase [57]. To examine correlation with the replication timing of CENP-A-associated DNA, I examined the co-localization of CENP-A dots and PCNA foci during the cell cycle. Figure 9B shows that CENP-A dots were co-localized with replication foci or aggregates of PCNA in mid S phase (1080 min) and late S phase (1560 min).

Figure 10A shows the representative fluorescent images of mKO-CENP-A and EGFP-PCNA in mid S phase (1032–1128 min), as shown in Fig. 8, but with 12 min intervals. First, I focused on CENP-A dots 2 and 10, located in the nuclear periphery and in the center of nucleus, respectively (see rectangle area in Fig. 10A). At the position of CENP-A dot 2, a distinct focus of PCNA was observed at 1044 min. It extended to the CENP-A dot 10 at 1056 min with small granules or aggregates until 1080 min. The PCNA focus at CENP-A dot 2 diffused at 1092 min and finally

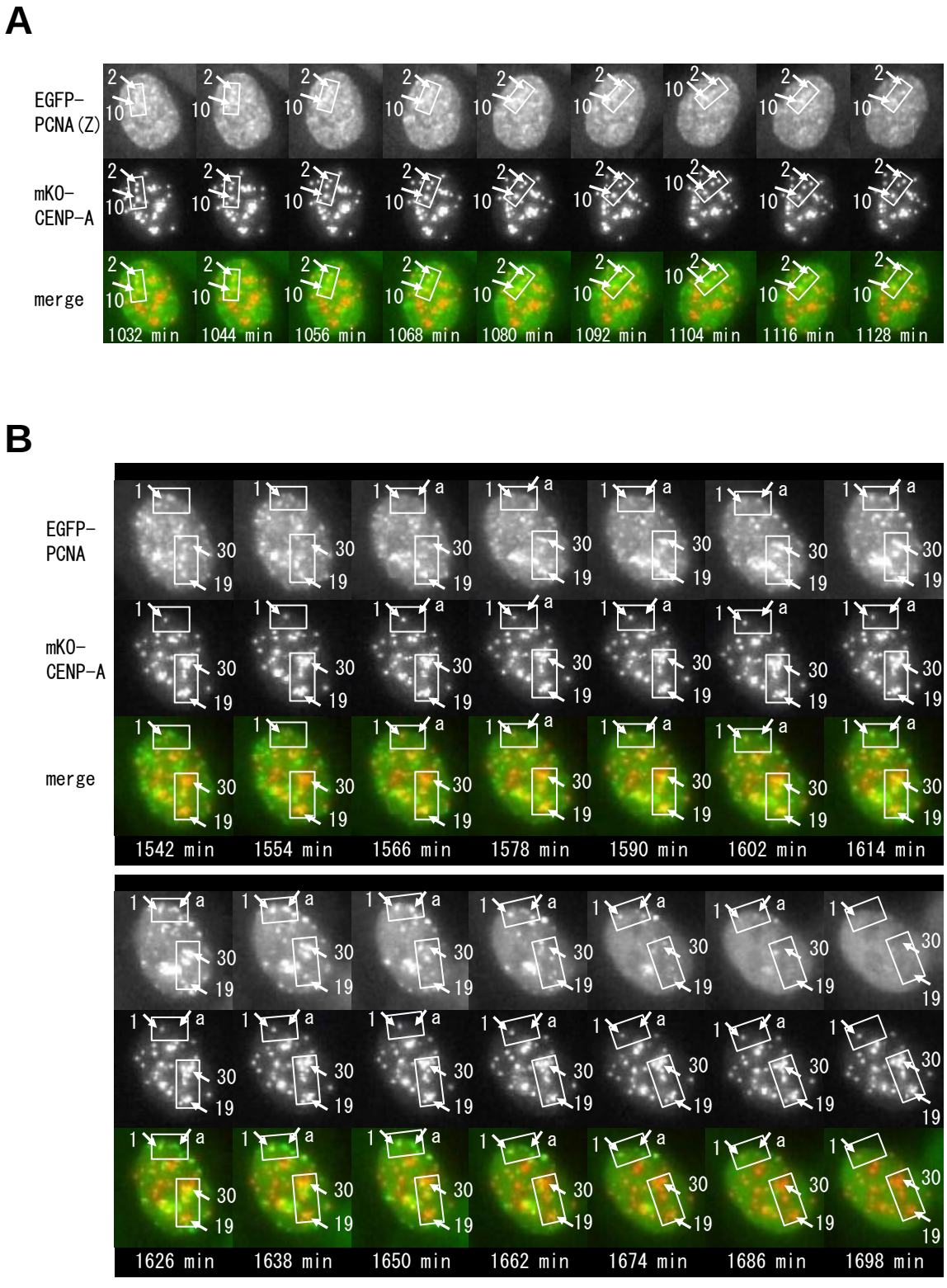

Fig. 10. For figure C and legend, see next page.

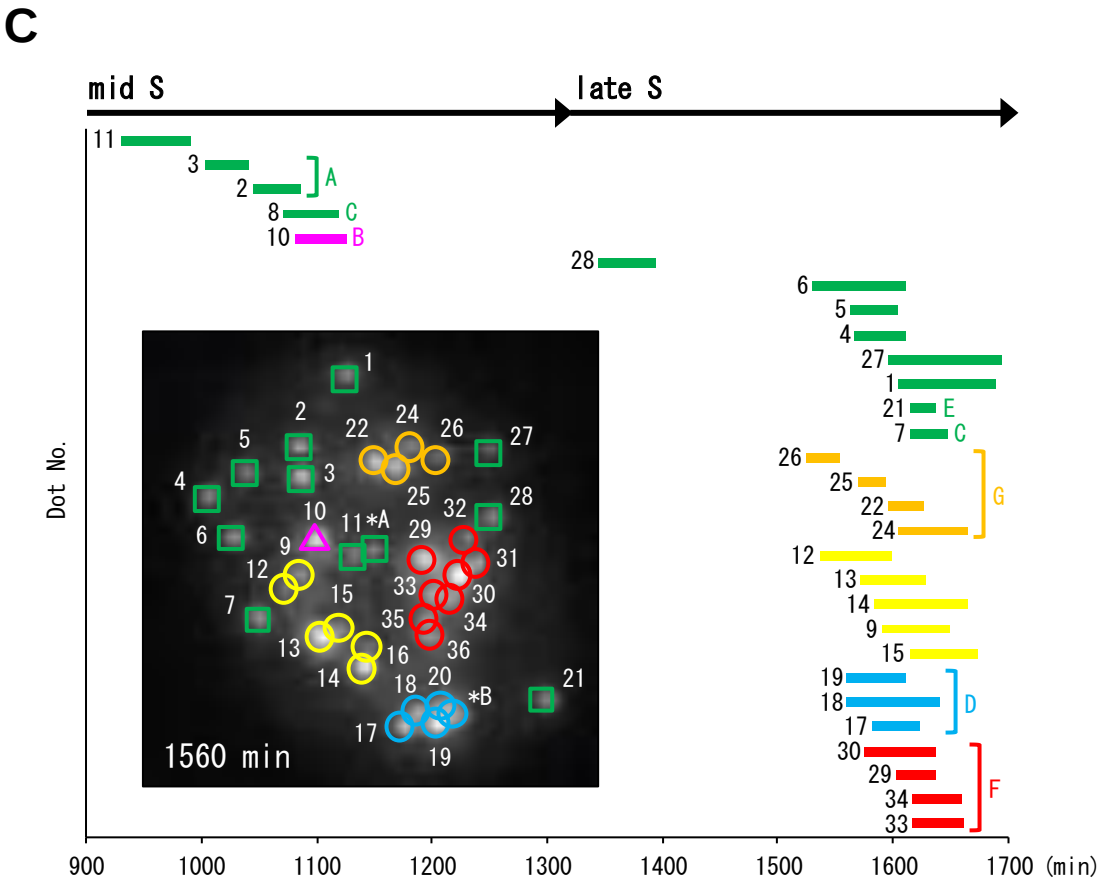

Fig. 10. Co-localization of CENP-A dots and PCNA foci in S phase.
A, **B**, Fluorescent images of mKO-CENP-A and EGFP-PCNA in HT1080 cell in S phase. Each image of mKO-CENP-A (orange) and EGFP-PCNA (green) of HT1080 cell was captured at 3 min intervals, but the representative images of mid S and late S phases are shown. The elapsed time after G1 phase onset (0 min) is indicated at the bottom. EGFP-PCNA (Z) shows the maximum-projection image of the serial Z-sections at each timepoint. **C**, Durations of the co-localization of CENP-A dots and PCNA foci. The localization of CENP-A dots, identified and numbered in Fig. 9A, was analyzed by the Z-stacks of the images of 1560 min (inset). CENP-A dots in the nuclear periphery are shown by green squares and magenta triangle, and those in the nucleoli are shown in yellow, cyan, orange, and red circles. CENP-A dots 8 and 23 are not shown in the inset since they could not be discriminated from CENP-A dots 12 and 22, respectively. The CENP-A dot numbers are shown on the left of each bar. Brackets A–G on the right indicate the same groups of CENP-A enclosed by circles A–G in Fig. 8. CENP-A dots *A and *B are not shown here, since they could not be discriminated from CENP-A dots 11 and 20, respectively.

disappeared at 1104 min, although the rest of foci or aggregates still remained in the vicinity of CENP-A dot 2. Thus, I concluded that the PCNA focus was co-localized with CENP-A dot 2 for 36 min (1044–1080 min). Similarly, the replication timing of CENP-A dot 10-associated DNA was estimated. No PCNA focus was observed at the position of CENP-A dot 10 at 1032 min. Instead, there were small granules between dot 2 and dot 10. They formed a distinct PCNA focus in the vicinity of CENP-A dot 10 at 1044 min and extended above at 1056 min, but was not co-localized with dot 10. A large aggregate of PCNA appeared at CENP-A dot 10 at 1080 min and its morphology changed from 1092 min to 1104 min. The co-localization of PCNA with CENP-A was observed until 1116 min for 36 min. Then the PCNA focus shifted above and left of the position of CENP-A dot 10 at 1128 min. Although PCNA foci changed their morphology, the relative position of four CENP-A dots in the rectangle area was maintained during this period (1032–1128 min).

Figure 10B shows the localization of mKO-CENP-A and EGFP-PCNA in late S phase. As shown within the upper rectangle, CENP-A dot 1 was localized in the nuclear periphery. Three replication foci in different sizes were found in this area. When carefully compared with CENP-A dot 1, these foci were not co-localized with CENP-A dot 1 and disappeared at 1566 min. At 1590 min, however, a cloud or amorphous shape of PCNA appeared around at CENP-A dot 1 and formed a replication focus at 1614 min. It enlarged in size, changing its morphology from 1626 to 1650 min, and became a discrete focus at 1650 min. The focus decreased in size at 1674 min and almost disappeared at 1686 min. The co-localization of PCNA with CENP-A dot 1 was observed for 72 min (1614–1686 min). During this period, another replication focus, without association with CENP-A dot, appeared in the upper nuclear periphery (indicated by ‘a’) at 1590 min and enlarged in size, changing its morphology between 1614–1650 min. It diffused between 1662–1674 min and disappeared at 1698 min.

Similarly, I characterized with CENP-A dots 19 and 30, which had been localized in the area of nucleoli (cyan and red lines, respectively, in Fig. 9) in G1 and early S

phases. As shown in the mKO-CENP-A panel of Fig. 10B, these CENP-A dots were located in the clusters of CENP-A dots are indicated within the lower rectangle. As shown in the EGFP-PCNA panel, 5 PCNA foci were identified in the same rectangle area. One in the middle was co-localized with the lower dot of the CENP-A doublet, but another was not (see yellow for the overlap and green for non-overlap in the merge panel). To precisely compare the spatial positions of these foci with CENP-A dots 30 and 19, I re-examined the Z-stacks of the image of 1542 min. I found that none of PCNA foci co-localized with CENP-A dots 30 and 19 at this time. Interestingly, the lowest PCNA focus moved to and co-localized with CENP-A dot 19 at 1554 min. It enlarged in size at 1566 min, changing its morphology until 1602 min, decreased in size at 1614 min and disappeared at 1626 min. The co-localization with CENP-A dot 19 continued for 48 min (1554–1602 min). Similar observations were seen with CENP-A dot 30. The upper PCNA foci shifted to CENP-A dot 30 at 1566 min, grew in size from 1578 min to 1638 min, and then disappeared at 1650 min. The co-localization of PCNA with CENP-A dot 30 continued for 60 min. The relative position of the CENP-A dots in the nucleus did not change much in late S phase (1542–1698 min). As the PCNA foci disappeared, the nucleolar exclusion pattern of PCNA was observed again (1674 min). I found that the clusters of CENP-A dots in the lower rectangle, including dots 19 and 30, were just localized in the nucleolar exclusion areas at 1698 min.

Figure 10C summarizes the durations of the co-localization of CENP-A dots with PCNA foci in mid and late S phases. No co-localization was observed in early S phase (data not shown). The inset shows the larger image of mKO-CENP-A of 1560 min shown in Fig. 9B. All CENP-A dots identified at 1080 min shown in Fig. 9A could be chased until G2 phase (1830 min), but were not always discriminated from each other. Thus, 29 of 36 CENP-A dots were assigned to be co-localized with PCNA foci, with 5 dots in mid S phase and 24 dots in late S phase. Thirteen CENP-A dots in the nuclear periphery, indicated by green and magenta bars, were located in mid and late S phases. Interestingly, the start of the co-localization of CENP-A dots 2 and 3 (group A) were

near to CENP-A dot 8 (group C), but were far from CENP-A dot 7 (group C). In contrast, the other dots in the nucleolar regions, indicated by orange, yellow, cyan, and red bars, were located in late S phase. These results indicated that CENP-A dots were co-localized with PCNA foci in late S phase, keeping the territory of CENP-A dots in the nucleus.

The duration of the co-localization with PCNA foci varied from CENP-A dot to dot, and from 24 min for the shortest (CENP-A dot 21, 25) to 99 min for the longest (CENP-A dot 27). There was no significant difference in the average of duration period between the nucleoli and the other region, 51.5 ± 17.1 min (n = 16) and 53.3 ± 21.9 min (n = 13), respectively, and was no significant difference in the average between mid S phase and late S phase, 46.8 ± 8.1 min (n = 5) and 53.5 ± 20.6 min (n = 24), respectively.

Territory of prekinetochore dots of mKO-CENP-A in interphase and co-localization with replication foci of EGFP-PCNA in S phase.

To confirm the territory of CENP-A dots in the nucleus and their co-localization with PCNA foci in late S phase, I analyzed the localization of mKO-CENP-A and EGFP-PCNA from late G1 phase through to late G2 phase in another cell (Fig. 11A). In late G1 and early S phases, the nucleolar exclusion pattern of PCNA was observed, indicating four nucleoli in these areas. To follow the positions in the cell cycle, the boundary of presumptive nucleoli was enclosed with yellow, red, orange, and cyan lines (from large to small ones in the EGFP-PCNA panel). The CENP-A dots positioned in the presumptive nucleoli in late G1 phase (-21 min) were grouped into yellow, red, orange, and cyan circles, and the others in the nuclear periphery were indicated by green squares. Each CENP-A dot was chased from late G1 phase to late G2 phase. The relative positions of CENP-A dots in interphase, not all but those characterized, are schematically presented in the upper panel of Fig. 11A. The results indicated that CENP-A dots well maintained their territory in the nucleus form G1 phase through G2

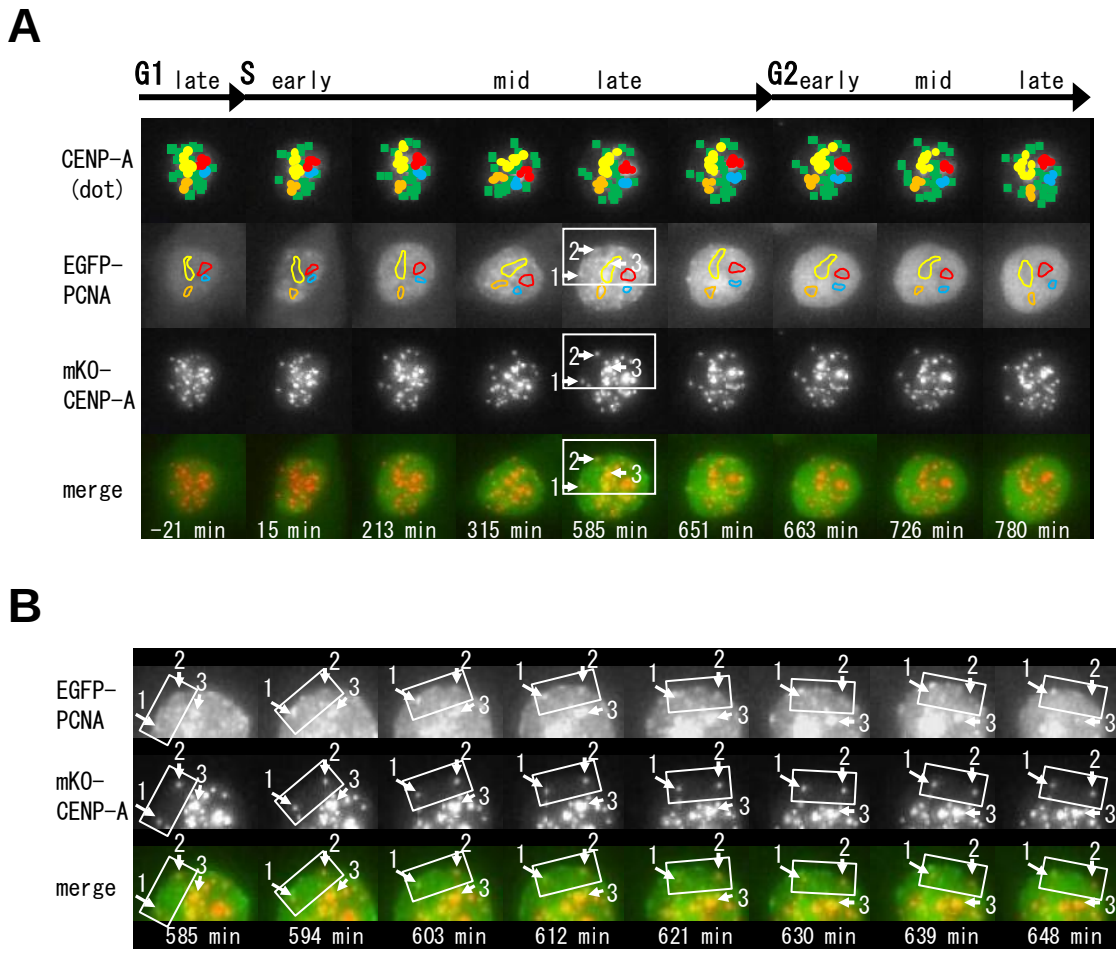

Fig. 11. Comparison of the localization pattern of CENP-A dots with the nucleolar exclusion pattern of PCNA in HT1080 cells.
A, Fluorescent images of mKO-CENP-A and EGFP-PCNA of another HT1080 cell from late G1 phase to late G2 phase. Each fluorescent image of CENP-A and PCNA was characterized as described in the Fig. 9 legend. The boundaries of four presumptive nucleoli at -21 min are shown in yellow, red, orange, and cyan lines (from large to small ones). CENP-A dots in the presumptive nucleoli were grouped into four and marked with yellow, red, orange, and cyan circles, according to the position, while those in the nuclear periphery are shown with green squares. Each CENP-A dot was chased from late G1 phase (-21 min) to late G2 phase (780 min) and the relative positions were shown in the upper panel in colors (CENP-A dot). In contrast, the relative positions of the nucleoli during the cell cycle, except for late S phase (585 min), were estimated by comparing the serial time-lapsed images of PCNA and shown in the EGFP-PCNA panel. **B**, Fluorescent images of mKO-CENP-A and EGFP-PCNA in late S phase. Each image of HT1080 cells stably expressing mKO-CENP-A (orange) and EGFP-PCNA (green) was captured at 3 min intervals. The elapsed time after S phase onset (0 min) is indicated at the bottom.

phase. In late S and G2 phases, the nucleolar exclusion pattern of PCNA was observed again. The four groups of CENP-A dots positioned in the nucleoli in late G1 phase were located in the corresponding nucleolar areas: yellow to yellow, red to red, orange to orange, and cyan to cyan (compare the upper CENP-A panel with the EFGP-PCNA panel).

Figure 11B shows the co-localization of the CENP-A dot 1-3 with PCNA in late S phase. As shown in the rectangle area, CENP-A dot 2 was co-localized with PCNA foci from 594 min to 639 min. The co-localization of CENP-A dot 1 and PCNA started at 573 min and finished at 612 min, while that of CENP-A dot 3 started at 579 min and finished at 630 min.

Comparison of the localization pattern of prekinetochore dots of mKO-CENP-A between parental and daughter cells.

Figure 12 shows the localization patterns of CENP-A dots in parental and two daughter cells. The typical nucleolar exclusion pattern was observed in the parental cell before the nuclear envelope breakdown (-30 min). There were three presumptive nucleoli. In M phase, PCNA was distributed in the cytoplasm, but the fluorescence of PCNA was weak in the chromosomal region where CENP-A was localized. As with chromosome de-condensation, PCNA was gradually concentrated into the nucleus and the nucleolar exclusion pattern appeared in daughter nuclei after 60 min in G1 phase and was maintained until early S phase (435 min and 420 min, in the upper and lower daughter cells, respectively). However, the distribution pattern of the presumptive nucleoli was different from that of the parental cell and between two daughter cells as well. Furthermore, the localization pattern of CENP-A dots in the parental cell did not seem to be maintained in either daughter cell.

As shown in the EGFP-PCNA panel, the boundary of presumptive nucleoli in daughter cells in early S phase (435 min and 420 min) was enclosed with yellow, red, orange, and cyan lines (from large to small ones). I followed the CENP-A dots in the

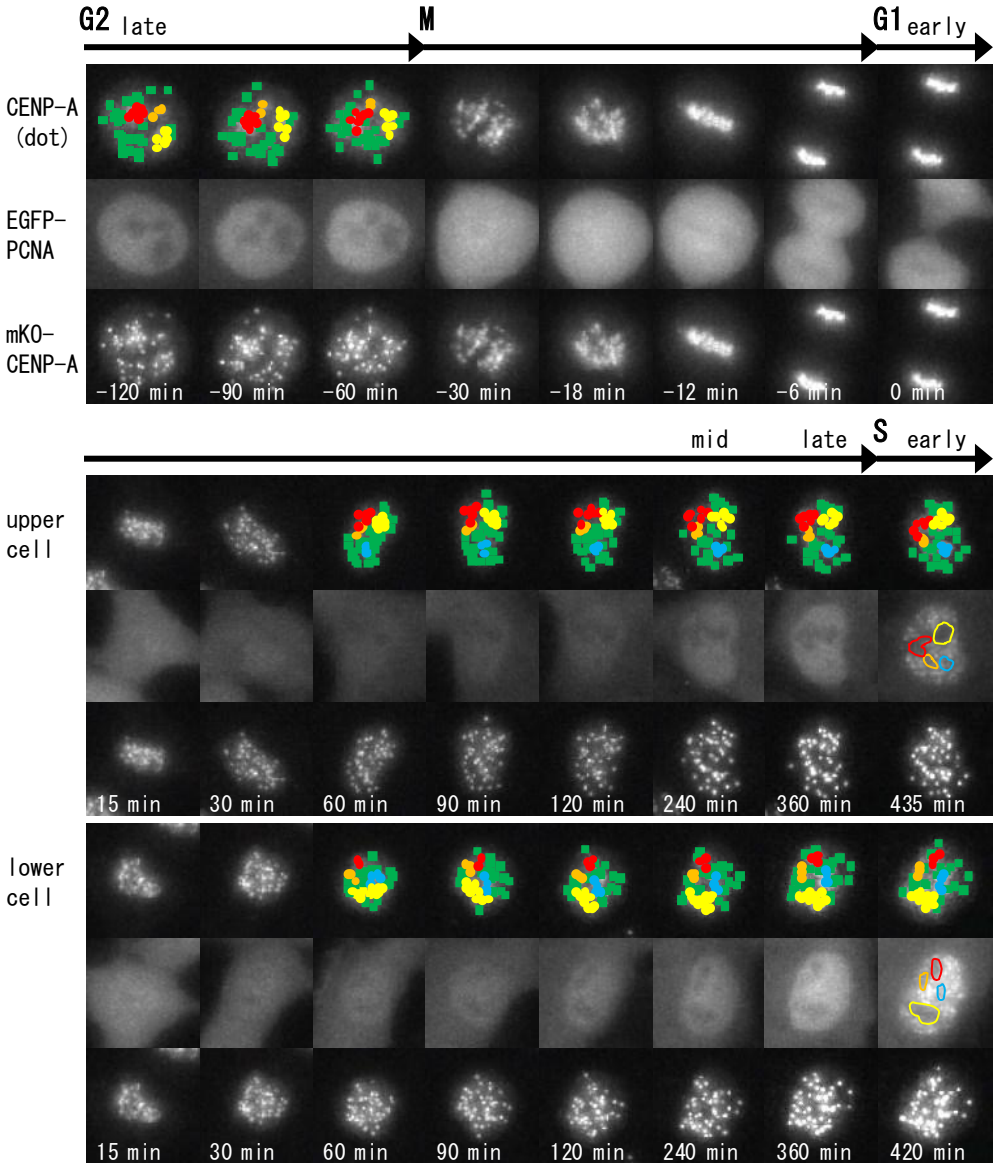

Fig. 12. Localization pattern of CENP-A dots and nucleolar exclusion pattern of PCNA among parental and daughter cells.
Each image of mKO-CENP-A (orange) and EGFP-PCNA (green) of another HT1080 cell was captured from late G2 phase through to early S phase at 3 min intervals. The elapsed time before and after G1 phase onset (0 min) is indicated at the bottom. CENP-A dots localized in the nuclear periphery are shown by green squares and those in the nucleoli are shown by yellow, cyan, orange, and red circles. The localization patterns of CENP-A dots and the nucleolar exclusion pattern of PCNA were different between daughter cells as well as among the parental cell and two daughter cells.

presumptive nucleoli (yellow, red, orange, and cyan circles) as well as the others in the nuclear periphery (green squares). After the cell division, the relative positions of CENP-A dots seemed to be fixed independently in the daughter nuclei and were maintained through G1 phase to early S phase.

DISCUSSION

Lidsky *et al.* [49] recently reported live cell imaging of *Drosophila* S2R+ cells stably expressing Cid/CENP-A-EGFP and mCherry-PCNA during the cell cycle. The nucleolar exclusion pattern of PCNA was also observed in these *Drosophila* cells. Two larger dots or aggregates of Cid/CENP-A appeared in early G1 phase and were located at the periphery of the nucleolus until early S phase. The co-localization of Cid/CENP-A and PCNA foci was observed at the nucleolar periphery in mid S phase, although the authors had not characterized it further.

In this Chapter II, I characterized the molecular behavior of human CENP-A and PCNA throughout the cell cycle. To express mKO-CENP-A and mCherry-PCNA, I used the HT1080 fibrosarcoma cell line with a modal number of 46 chromosomes and a few chromosomal changes from the normal diploid karyotype [54]. By capturing 15 optical Z-sections of the live cell images at 3 min intervals, more than half of the CENP-A dots could be chased from early G1 phase to late G2 phase (see Figs. 8 and 9). I found that most CENP-A dots were co-localized with PCNA foci in mid and late S phases (Fig. 10), probably reflecting the replication process of CENP-A-associated DNA in the living state. The localization pattern of CENP-A dots was further compared with the nucleoli indicated by the nucleolar exclusion pattern of PCNA in G1, early S, and G2 phases [40, 55, 58, 59]. CENP-A dots were localized in the nucleoli as well as in the nuclear periphery, and their relative positions hardly changed during interphase in HT1080 cells (Fig. 11).

Sugimoto *et al.* [48] showed that EGFP-fused CENP-A was co-localized with

endogenous CENP-C in human MDA435 cells. Hemmerich *et al.* [51] reported FRAP experiments with human HEp-2 cells expressing GFP-CENP-C and mRFP-PCNA. The authors showed that some CENP-C dots were also localized in the nucleoli and in the nuclear periphery from early S phase thorough to late S phase (see Fig. 4 of [51]), although they did not follow them through the cell cycle. Carroll *et al.* found that CENP-C and CENP-N bind directly to CENP-A nucleosomes in the assembly of kinetochore [60, 61]. Hellwig *et al.* [52] further characterized the localization of EGFP-CENP-N and mRFP-PCNA in HEp-2 cells and found that the majority of CENP-N is loaded at the kinetochores during S phase but dissociates during G2 phase. The authors showed that CENP-N dots were localized in the nucleoli and in the nuclear periphery in mid S phase. Therefore, the association of these CENP dots with the nucleoli might be important for kinetochore assembly.

The localization pattern of CENP-A dots was different between parental and daughter HT1080 cells (see Fig. 12). The number and morphology of the nucleoli in daughter cells were not comparable to that in parental cells as well. After cell division, the localization pattern of CENP-A dots may be fixed by their relative position of each chromosome in daughter nuclei in early G1 phase. The chromosome analysis of HT1080 cells showed a modal number of 46 chromosomes with a distribution between 44 and 48 [54]. Chromosome mis-segregations will change the localization pattern of CENP-A dots in daughter nuclei. If a certain chromosome, by chance, delays in the chromosome segregation process, the relative position of other CENP-A dots would be affected by the chromosome that is slightly left behind in daughter nuclei. Furthermore, it may be affected by the asymmetry of the mitotic spindle or spindle poles, somehow disturbed in the parental cells. It will be interesting to examine whether the relative position of CENP-A dots is maintained throughout the cell cycle in non-transformed cell lines or primary cells with normal karyotype.

In humans, rDNA genes are mapped on the short arms of chromosomes 13, 14, 15, 21, and 22. Nucleoli are formed around the nucleolus organizer regions (NORs) [62].

Thus, centromeres of these acrocentric chromosomes should be located close to the nucleoli in interphase. In fact, Németh *et al.* [56] showed that certain centromeres were located at nucleolus-associated chromatin domains (NADs) in HeLa cells. My results also indicated that more than 10 CENP-A dots were localized in the nucleolar regions in HT1080 cells (see Fig. 9). The association of CENP-A dots with nucleoli may contribute to the subnuclear organization of chromosomes, as described by van Koningsbruggen *et al.* (see Fig. 10 of [63]). Assembly of nucleolus starts in telophase and is completed in early G1 phase [64]. The nucleolar exclusion pattern of PCNA was observed 60 min after the cell division (see Fig. 8). Muro *et al.* [65] reported that the nucleolar assembly was completed within 120 min in HeLa cells. Thus, the localization pattern of CENP-A dots may be correlated with the timing of the nucleolar assembly in early G1 phase. Further studies are needed to elucidate how the localization pattern of CENP-A dots is determined in early G1 phase.

CONCLUSIONS

In eukaryote, the cell cycle is divided into G1, S, G2, and M phases. DNA is synthesized in S phase, and chromosome segregation and cell division are occurred in M phase (mitosis and cytokinesis, respectively). Events of the cell cycle occur in the correct sequence. For understanding of life phenomena, visualization of the progression of the cell cycle by using specific proteins and spatiotemporal observation of the molecular behavior of the proteins are important. So far, the living cell marker throughout the cell cycle that can be easily used only by observing the specific localization of the protein is unknown. Therefore, the protein that changes the localization in interphase may be a candidate as a marker of all cell cycle phases. In this thesis, I focus on the molecular behavior of the proteins that may change the localization in interphase in living cells.

In CHAPTER I, I characterized the molecular behavior of HP1α throughout the cell cycle in mouse C3H10T1/2 cells. I found that interphase was divided into four phases, Phases 1–4, by characterizing the localization of HP1α by the long-term live-cell imaging. In Phase 1, HP1α formed heterochromatin dots soon after the first cell division, typical of its localization during interphase [18, 19, 25]. In Phase 2, HP1α began to diffuse into the nucleoplasm and its diffusion increased gradually. In Phase 3, HP1α diffused further towards the nuclear periphery. In Phase 4, HP1α was uniformly distributed in the nucleus, and then the cells entered into M phase. Therefore, HP1α may be useful as an interphase living cell marker at least in mouse cells. The localization of HP1α dynamically changes in the middle of interphase. In Phase 2, the diffusion of HP1α in the nucleoplasm started and the fluorescence intensity of HP1α dots changed periodically. The fluorescence intensity increased independently of the periodic change in the fluorescence intensity of HP1α dots, suggesting that the diffusion of HP1α in the nucleoplasm was not caused by the degradation of HP1α dots but caused by the increase of the enhanced expression of HP1α in the nucleoplsm. Therefore, it is likely that Phase

2 may overlap with S phase. Further studies are required to determine the exact timing and to elucidate the molecular mechanism underlying the flickering of HP1α dots.

In CHAPTER II, I characterized the molecular behavior of human CENP-A and PCNA throughout the cell cycle in human HT1080 cells. The localization pattern of CENP-A dots was compared with the nucleoli indicated by the nucleolar exclusion pattern of PCNA in G1, early S, and G2 phases [40, 55, 58, 59]. I found that CENP-A dots were localized in the nucleoli as well as in the nuclear periphery, and their relative positions hardly changed during interphase in HT1080 cells. Therefore, the pattern of CENP-A dots may be useful for the positioning of the localization of other proteins. I further found that most CENP-A dots in the nucleoli and the nuclear periphery were co-localized with PCNA foci in late S phase, while some CENP-A dots in the nuclear periphery were co-localized in mid S phase. These results probably reflecting the replication process of CENP-A-associated DNA in the living state.

REFERENCES

[1] Nurse, P. (2000) A long twentieth century of the cell cycle and beyond. *Cell*, **100**, 71–78.

[2] Hartwell, L.H., and Weinert, T.A. (1989) Checkpoints: controls that ensure the order of cell cycle events. *Science*, **246**, 629–634.

[3] Leonhardt, H., Page, A.W., Weier, H.U., and Bestor, T.H. (1992) A targeting sequence directs DNA methyltransferase to sites of DNA replication in mammalian nuclei. *Cell*, **71**, 865–873.

[4] Cardoso, M.C., Joseph, C., Rahn, H.P., Reusch, R., Nardal-Ginard, B., and Leonhardt, H. (1997) Mapping and use of a sequence that targets DNA ligase I to sites of DNA replication in vivo. *J. Cell Biol.*, **139**, 579–587.

[5] Celis, J.E., and Celis, A. (1985) Cell cycle-dependent variations in the distribution of the nuclear protein cyclin proliferating cell nuclear antigen in cultured cells: subdivision of S phase. *Proc. Natl. Acad. Sci. USA*, **82**, 3262–3266.

[6] Easwaran, H.P., Schermelleh, L., Leonhardt, H., and Cardoso, M.C. (2004) Replication-independent chromatin loading of Dnmt1 during G2 and M phases. *EMBO Rep.*, **5**, 1181–1186.

[7] Easwaran, H.P., Leonhardt, H., and Cardoso, M.C. (2005) Cell cycle markers for live cell analyses. *Cell Cycle*, **4**, 453–455.

[8] Ersoy, I., Bunyak, F., Chagin, V., Cardoso, M.C., and Palaniappan, K. (2009) Segmentation and classification of cell cycle phases in fluorescence imaging. *Lect. Notes Comput. Sci.*, **5762**, 617–624.

[9] James, T.C. and Elgin, S.C. (1986) Identification of a nonhistone chromosomal protein associated with heterochromatin in *Drosophila melanogaster* and its gene. *Mol. Cell. Biol.*, **6**, 3862–3872.

[10] Eissenberg, J.C., James, T.C., Foster-Hartnett, D.M., Hartnett, T., Ngan, V., and

Elgin, S.C. (1990) Mutation in a heterochromatin-specific chromosomal protein is associated with suppression of position-effect variegation in *Drosophila melanogaster*. *Proc. Natl. Acad. Sci. USA*, **87**, 9923–9927.

[11] Lorentz, A., Ostermann, K., Fleck, O., and Schmidt, H. (1994) Switching gene *swi6*, involved in repression of silent mating-type loci in fission yeast, encodes a homologue of chromatin-associated proteins from *Drosophila* and mammals. *Gene*, **143**, 139–143.

[12] Smothers, J.F., and Henikoff, S. (2001) The hinge and chromo shadow domain impart distinct targeting of HP1-like proteins. *Mol. Cell. Biol.*, **21**, 2555–2569.

[13] Saunders, W.S., Chue, C., Goebl, M., Craig, C., Clark, R.F., Powers, J.A., Eissenberg, J.C., Eglin, S.C., Rothfield, N.F., and Earnshaw, W.C. (1993) Molecular cloning of a human homologue of *Drosophila* heterochromatin protein HP1 using anti-centromere autoantibodies with *anti-chromo* specificity. *J. Cell Sci.*, **104**, 573–582.

[14] Furuta, K., Chan, E.K.L., Kiyosawa, K., Reimer, G., Luderschmidt, C., and Tan, E.M. (1997) Heterochromatin protein $HP1^{Hs\beta}$ (p25β) and its localization with centromeres in mitosis. *Chromosoma*, **106**, 11–19.

[15] Ye, Q., and Worman, H.J. (1996) Interaction between an integral protein of the nuclear envelope inner membrane and human chromodomain proteins homologous to *Drosophila* HP1. *J. Biol. Chem.*, **271**, 14653–14656.

[16] Paro, R., and Hogness, D.S. (1991) The Polycomb protein shares a homologous domain with a heterochromatin-associated protein of *Drosophila*. *Proc. Natl. Acad. Sci. USA*, **88**, 263–267.

[17] Aasland, R., and Stewart, A.F. (1995) The chromo shadow domain, a second chromo domain in heterochromatin-binding protein 1, HP1. *Nucleic. Acids. Res.*, **23**, 3168–3173.

[18] Yamada, T., Fukuda, R., Himeno, M., and Sugimoto, K. (1999) Functional domain structure of human heterochromatin protein $HP1^{Hs\alpha}$: involvement of

internal DNA-binding and C-terminal self-association domains in the formation of discrete dots in interphase nuclei. *J. Biochem.*, **125**, 832–837.

[19] Minc, E., Allory, Y., Worman, H.J., Courvalin, J.C., and Buendia, B. (1999) Localization and phosphorylation of HP1 proteins during the cell cycle in mammalian cells. *Chromosoma*, **108**, 220–234.

[20] Minc, E., Courvalin, J.C., and Buendia, B. (2000) HP1gamma associates with euchromatin and heterochromatin in mammalian nuclei and chromosomes. *Cytogenet. Cell Genet.*, **90**, 279–284.

[21] Wong, A.K., and Rattner, J.B. (1988) Sequence organization and cytological localization of the minor satellite of mouse. *Nucleic Acids Res.*, **16**, 11645–11661.

[22] Joseph, A., Mitchell, A.R., and Miller, O.J. (1989) The organization of the mouse satellite DNA at centromeres. *Exp. Cell Res.*, **183**, 494–500.

[23] Matsuda, Y., and Chapman, V.M. (1991) In situ analysis of centromeric satellite DNA segregating in *Mus* species crosses. *Mamm.Genome*, **1**, 71–77.

[24] Guenatri, M., Bailly, D., Maison, C., and Almouzni, G. (2004) Mouse centric and pericentric satellite repeats form distinct functional heterochromatin. *J. Cell Biol.*, **166**, 493–505.

[25] Sugimoto, K., Tasaka, H., and Dotsu, M. (2001) Molecular behavior in living mitotic cells of human centromere heterochromatin protein HP1α ectopically expressed as a fusion to red fluorescent protein. *Cell Struct. Funct.*, **26**, 705–718.

[26] Sugimoto, K., Urano, T., Zushi, H., Inoue, K., Tasaka, H., Tachibana, M., and Dotsu, M. (2002) Molecular dynamics of Aurora-A kinase in living mitotic cells simultaneously visualized with histone H3 and nuclear membrane protein importin α. *Cell Struct. Funct.*, **27**, 457–467.

[27] Sugimoto, K., and Tone, S. (2010) Imaging of mitotic cell division and apoptotic intra-nuclear processes in multicolor. Live Cell Imaging, Methods

and Protocols. In: Papkovsky, D.B., editor. Humana Press, New York, NY, pp. 135–146.

[28] Nakagawa, C., Nishimura, S., Senda-Murata, K., and Sugimoto, K. (2012) A rapid and simple method of evaluating the dimeric tendency of fluorescent proteins in living cells using a truncated protein of importin α as fusion tag. *Biosci. Biotechnol. Biochem.*, **76**, 388–390.

[29] Sakaushi, S., Senda-Murata, K., Fukada, T., Oka, S., and Sugimoto, K. (2007) Rhythmic cycle of clathrin-coated pit formation at the *trans*-golgi network in human MDA-MB-435 cells. *Biosci. Biotechnol. Biochem.*, **71**, 571–574.

[30] Sakaushi, S., Inoue, K., Zushi, H., Senda-Murata, K., Fukada, T., Oka, S., and Sugimoto, K. (2007) Dynamic behavior of FCHO1 revealed by live-cell imaging microscopy: its possible involvement in clathrin-coated vesicle formation. *Biosci. Biotechnol. Biochem.*, **71**, 1764–1768.

[31] Aagaard, L., Laible, G., Selenko, P., Schmid, M., Dorn, R., Schotta G., Kuhfittig, S., Wolf, A., Lebersorger, A., Singh, P.B., Reuter, G., and Jenuwein, T. (1999) Functional mammalian homologues of the Drosophila PEV-modifier *Su(var)3-9* encode centromere-associated proteins which complex with the heterochromatin component M31. *EMBO J.*, **18**, 1923–1938.

[32] Nielsen, A.L., Sanchez, C., Ichnose, H., Cerviño, M., Lerouge, T., Chambon, P., and Losson, R. (2002) Selective interaction between the chromatin-remodeling factor BRG1 and the heterochromatin-associated protein HP1α. *EMBO J.*, **21**, 5797–5806.

[33] Daujat, S., Zeissler, U., Waldmann, T., Happel, N., and Schneider, R. (2005) HP1 binds specifically to Lys^{26}-methylated histone H1.4, whereas simultaneous Ser^{27} phosphorylation blocks HP1 binding. *J. Biol. Chem.*, **280**, 38090–38095.

[34] Schmiedeberg, L., Weisshart, K., Diekmann, S., Meyer zu Hoerste, G., and Hemmerich, P. (2004) High- and low-mobility populations of HP1 in

heterochromatin of mammalian cells. *Mol. Biol. Cell*, **15**, 2819–2833.

[35] Krouwels, I.M., Wiesmeijer, K., Abraham, T.E., Molenaar, C., Verwoerd, N.P., Tanke, H.J., and Dirks, R.W. (2005) A glue for heterochromatin maintenance: stable SUV39H1 binding to heterochromatin is reinforced by the SET domain. *J. Cell Biol.*, **170**, 537–549.

[36] Fujita, N., Watanabe, S., Ichimura, T., Tsuruzoe, S., Shinkai, Y., Tachibana, M., Chiba, T., and Nakao, M. (2003) Methyl-CpG binding domain 1 (MBD1) interacts with the Suv39h1-HP1 heterochromatic complex for DNA methylation-based transcriptional repression. *J. Biol. Chem.*, **278**, 24132–24138.

[37] Fuks, F., Hurd, P.J., Deplus, R., and Kouzarides, T. (2003) The DNA methyltransferases associate with HP1 and the SUV39H1 histone methyltransferase. *Nucleic Acids Res.*, **31**, 2305–2312.

[38] Stewart, M.D., Li, J., and Wong, J. (2005) Relationship between histone H3 lysine 9 methylation, transcription repression, and heterochromatin protein 1 recruitment. *Mol. Cell. Biol.*, **25**, 2525–2538.

[39] Chagin, V.O., Stear, J.H., and Cardoso, M.C. (2010) Organization of DNA replication. *Cold Spring Harb. Perspect. Biol.*, **2**, a000737.

[40] Amor, D.J., Bentley, K., Ryan, J., Perry, J., Wong, L., Slater, H., and Choo, K.H.A. (2004) Human centromere repositioning “in progress”. *Proc. Natl. Acad. Sci. USA*, **101**, 6542–6547.

[41] Palmer, D.K., O’Day, K., Trong, H.L., Charbonneau, H., and Margolis, R.L. (1991) Purification of the centromere-specific protein CENP-A and demonstration that it is a distinctive histone. *Proc. Natl. Acad. Sci. USA*, **88**, 3734–3738.

[42] Yoda, K., Ando, S., Morishita, S., Houmura, K., Hashimoto, K., Takeyasu, K., and Okazaki, T. (2000) Human centromere protein A (CENP-A) can replace histone H3 in nucleosome reconstitution *in vitro*. *Proc. Natl. Acad. Sci. USA*,

97, 7266–7271.

[43] Earnshaw, W.C., and Rothfield, N. (1985) Identification of a family of human centromere proteins using autoimmune sera from patients with scleroderma. *Chromosoma*, **91**, 313–321.

[44] Palmer, D.K., O'Day, K., Wener, M.H., Andrews, B.S., and Margolis, R.L. (1987) A 17-kD centromere protein (CENP-A) copurifies with nucleosome core particles and with histones. *J. Cell Biol.*, **104**, 805–815.

[45] Jansen, L.E.T., Black, B.E., Foltz, D.R., and Cleveland, D.W. (2007) Propagation of centromeric chromatin requires exit from mitosis. *J. Cell Biol.*, **176**, 795–805.

[46] Dunleavy, E.M., Almouzni, G., and Karpen, G.H. (2011) H3.3 is deposited at centromeres in S phase as a placeholder for newly assembled CENP-A in G_1 phase. *Nucleus*, **2**, 146–157.

[47] Bodor, D.L., Valente, L.P., Mata, J.F., Black, B.E., and Jansen, L.E.T. (2013) Assembly in G1 phase and long-term stability are unique intrinsic features of CENP-A nucleosomes. *Mol. Biol. Cell.*, **24**, 923–932.

[48] Sugimoto, K., Fukuda, R., and Himeno, M. (2000) Centromere/kinetochore localization of human centromere protein A (CENP-A) exogenously expressed as a fusion to green fluorescent protein. *Cell Struct. Funct.*, **25**, 253–261.

[49] Lidsky, P.V., Sprenger, F., and Lehner, C.F. (2013) Distinct modes of centromere protein dynamics during cell cycle progression in *Drosophila* S2R+ cells. *J. Cell Sci.*, **126**, 4782–4793.

[50] Krishna, T.S.R., Kong, X.P., Gary, .S, Burgers, P.M., and Kuriyan, J. (1994) Crystal structure of the eukaryotic DNA polymerase processivity factor PCNA. *Cell*, **79**, 1233–1243.

[51] Hemmerich, P., Weidtkamp-Peters, S., Hoischen, C., Schmiedeberg, L., Erliandri, I., and Diekmann, S. (2008) Dynamics of inner kinetochore assembly and maintenance in living cells. *J. Cell Biol.*, **180**, 1101–1114.

[52] Hellwig, D., Emmerth, S., Ulbricht, T., Döring, V., Hoischen, C., Martin, R., Samora, C.P., McAinsh, A.D., Carroll, C.W., Straight, A.F., Meraldi, P., and Diekmann, S. (2011) Dynamics of CENP-N kinetochore binding during the cell cycle. *J. Cell Sci.*, **124**, 3871–3883.

[53] Rasheed, S., Nelson-Rees, W.A., Toth, E.M., Arnstein, P., and Gardner, M.B. (1974) Characterization of a newly derived human sarcoma cell line (HT-1080). *Cancer*, **33**, 1027–1033.

[54] Sugimoto, K., Murata, K.S., and Oka, S. (2008) Construction of three quadruple-fluorescent MDA435 cell lines that enable monitoring of the whole chromosome segregation process in the living state. *Mut. Res.*, **657**, 56–62.

[55] Leonhardt, H., Rahn, H.P., Weinzierl, P., Sporbert, A., Cremer, T., Zink, D., and Cardoso, M.C. (2000) Dynamics of DNA replication factories in living cells. *J. Cell Biol.*, **149**, 271–279.

[56] Németh, A., Conesa, A., Santoyo-Lopez, J., Medina, I., Montaner, D., Péterfia, B., Solovei, I., Cremer, T., Dopazo, J., and Längst, G. (2010) Initial Genomics of the human nucleous. *PLoS Genet.*, **6**, e1000889.

[57] Shelby, R.D., Monier, K., and Sullivan, K.F. (2000) Chromatin assembly at kinetochores is uncoupled from DNA replication. *J. Cell Biol.*, **151**, 1113–1118.

[58] Trembecka-Lucas, D.O., and Dobrucki, J.W. (2012) A heterochromatin protein 1 (HP1) dimer and a proliferating cell nuclear antigen (PCNA) protein interact in vivo and are parts of a multiprotein complex involved in DNA replication and DNA repair. *Cell Cycle*, **11**, 2170–2175.

[59] Burgess, A., Lorca, T., and Castro, A. (2012) Quantitative live imaging of endogenous DNA replication in mammalian cells. *PLoS One*, **7**, e45726.

[60] Carroll, C.W., Milks, K.J., and Straight, A.F. (2010) Dual recognition of CENP-A nucleosomes is required for centromere assembly. *J. Cell Biol.*, **189**, 1143–1155.

[61] Carroll, C.W., Silva, M.C.C., Godek, K.M., Jansen, L.E.T, and Straight, A.F. (2009) Centromere assembly requires the direct recognition of CENP-A nucleosomes by CENP-N. *Nat. Cell Biol.*, **11**, 896–902.

[62] McStay, B., and Grummt, I. (2008) The epigenetics of rRNA genes: from molecular to chromosome biology. *Annu. Rev. Cell Dev. Biol.*, **24**, 131–157.

[63] van Koningsbruggen, S., Gierliński, M., Schofield, P., Martin, D., Barton, G.J., Ariyurek, Y., den Dunnen, J.T., and Lamond, A.I. (2010) High-resolution whole-genome sequencing reveals that specific chromatin domains from most human chromosomes associate with nucleoli. *Mol. Biol. Cell.*, **21**, 3735–3748.

[64] Hernandez-Verdun, D. (2011) Assembly and disassembly of the nucleolus during the cell cycle. *Nucleus*, **2–3**, 189–194.

[65] Muro, E., Gébrane-Younès, J., Jobart-Malfait, A., Louvet, E., Roussel, P., and Hernandez-Verdun, D. (2010) The traffic of proteins between nucleolar organizer regions and prenucleolar bodies governs the assembly of the nucleolus at exit of mitosis. *Nucleus*, **1–2**, 202–211.

PUBLICATIONS

1. Nakagawa, C., Kawakita, A., Fukada, T., and Sugimoto, K. (2014) Live-cell imaging of HP1α throughout the cell cycle of mouse C3H10T1/2 cells and rhythmical flickering of heterochromatin dots in interphase. *Biosci. Biotechnol. Biochem.*, **78**, 556–564.

2. Nakagawa, C., Murata, K., Kawakita, A., Fukada, T., and Sugimoto, K. (2015) Molecular behavior of CENP-A and PCNA throughout the cell cycle in living human HT1080 cells., in preparation.

OTHER PUBLICATIONS

1. Nakagawa, C., Inahata, K., Nishimura, S., and Sugimoto, K. (2011) Improvement of a Venus-based bimolecular fluorescence complementation assay to visualize bFos-bJun interaction in living cells. *Biosci. Biotechnol. Biochem.*, **75**, 1399–1401.

2. Nakagawa, C., Nishimura, S., Senda-Murata, K., and Sugimoto, K. (2012) A rapid and simple methods of evaluating the dimeric tendency of fluorescent proteins in living cells using a truncated protein of importin α as fusion tag. *Biosci. Biotechnol. Biochem.*, **76**, 388–390.

ACKNOWLEDGEMENTS

I would like to express the deepest appreciation to Dr. Kenji Sugimoto, professor of Osaka Prefecture University, for his kind guidance and encouragement throughout this study.

I would like to express my deep gratitude to Dr. Takashi Inui and Dr. Shinji Tanimori, professor of Osaka Prefecture University, for their valuable advices.

I am deeply grateful to Dr. Takashi Fukada, assistant professor of Osaka Prefecture University, for his useful discussions and advices.

I also thank to past and present members of the Laboratory of Applied Molecular Biology of Osaka Prefecture University.